Dr. 1948-8

DOE/SF/10816-T1
(DE83013419)

RESIDENTIAL COOLING BY NOCTURNAL RADIATION

Passive Cooling Experimental Facility Hot/Arid Zone

By
T. L. Thompson

May 1983

Work Performed Under Contract No. AC03-80SF10816

University of Arizona
Tucson, Arizona

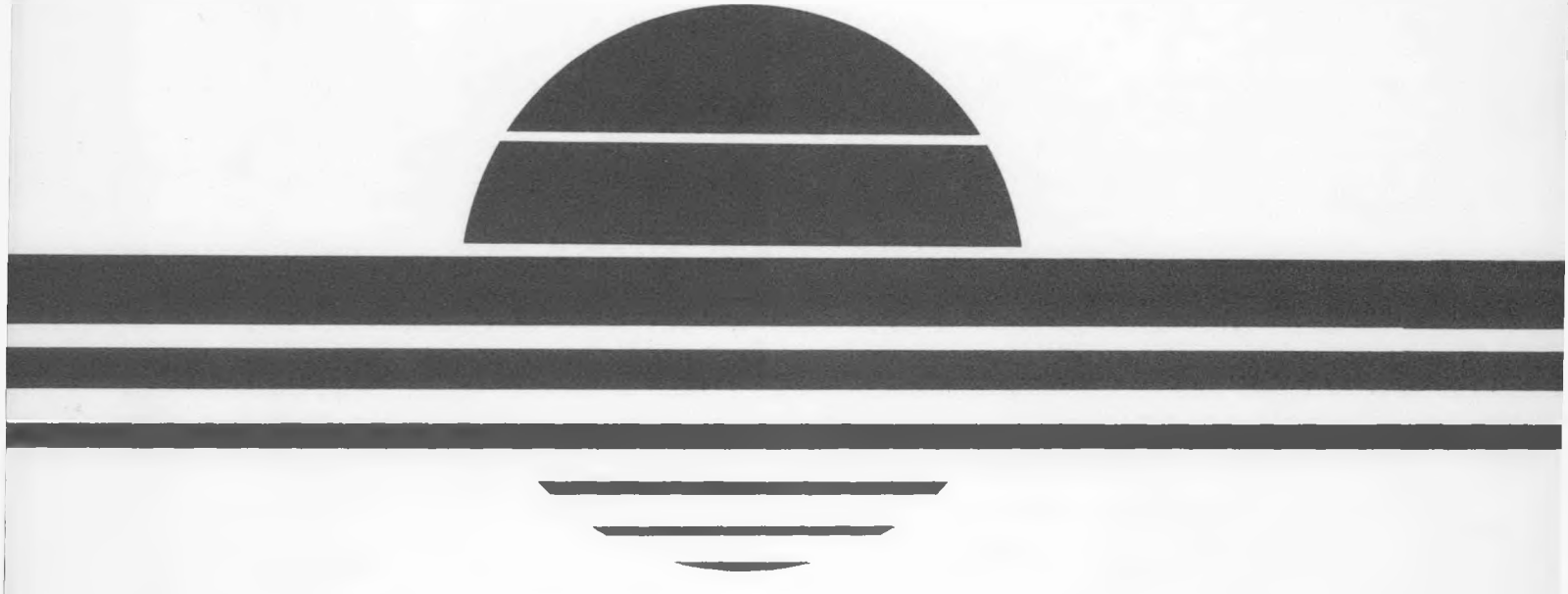

U.S. Department of Energy

Solar Energy

DISCLAIMER

This report has been reproduced directly from the best available copy.

Available from the National Technical Information Service, U. S. Department of Commerce, Springfield, Virginia 22161.

Price: Printed Copy A05
Microfiche A01

Codes are used for pricing all publications. The code is determined by the number of pages in the publication. Information pertaining to the pricing codes can be found in the current issues of the following publications, which are generally available in most libraries: *Energy Research Abstracts (ERA); Government Reports Announcements* and Index (*GRA* and I); *Scientific and Technical Abstract Reports (STAR);* and publication NTIS-PR-360 available from NTIS at the above address.

Printed in the United States of America
USDOE Technical Information Center, Oak Ridge, Tennessee

DOE/SF/10816-T1
(DE83013419)
Distribution Category UC-59a

Passive Cooling Experimental Facility

Hot/Arid Zone

Contract No. DE-AC03-805F-10816

RESIDENTIAL COOLING BY NOCTURNAL RADIATION

T. L. Thompson

Prepared for the Department of Energy

May, 1983

Environmental Research Laboratory

University of Arizona

Tucson International Airport

Tucson, Arizona 85706

Table of Contents

List of Illustrations

Definition of Terms

A Intensity of atmospheric radiation on a horizontal surface, Btu/sq ft hr.

A_f Active area of roof, under which fluid is flowing, sq ft.

A_r Total roof area, sq ft.

c_{pf} Specific heat of circulating fluid, Btu/lb ^{o}F.

c_s Heat capacity of one lb of dry air and the moisture it contains, Btu/(^{o}F)(lb dry air).

F_R Collector (roof) plate efficiency factor; F_{Rw}, efficiency factor for a wet roof.

G Flow rate of circulating fluid per unit area of active roof, lb/sq ft hr.

H Absolute humidity, $lb_{water}/lb_{dry\ air}$; H_a, of ambient air; H_m, of saturated air at the outside metal temperature.

h Heat transfer coefficient, Btu/sq ft hr ^{o}F; h_{ci}, inside convective coefficient; h_{co}, outside convective coefficient; h_o, combined outside convective and radiative coefficient for

a dry roof; h_{ow}, combined outside convective and radiative coefficient for a wet roof; and h_r, equivalent radiative heat transfer coefficient.

i Enthalpy of air, Btu/$lb_{dry\ air}$; i_a, of ambient or outdoor air; and i_m, of saturated air at the outside metal temperature.

k_{co} Mass transfer coefficient, lb/(hr)(sq ft)(unit ΔH).

k_m Thermal conductivity of fin material, Btu/ft hr ^{o}F.

L Length of flow channel in roof, ft.

ℓ Fin length from root to center, ft.

m Term appearing in fin effectiveness equation, ft^{-1}.

m_f Flow rate of circulating fluids, lb/hr.

N_t Number of transfer units.

Q Rate of heat transfer, Btu/hr ft.

q Heat transfer rate per unit roof area, Btu/sq ft hr; q_A, total

solar radiation heat absorption rate; q_s, incident solar radiation on roof; q_u, useful heat absorption or rejection rate.

R — Net radiation from a thermally black, horizontal plane at air temperature to the sky, Btu/sq ft hr.

R_b — Bond resistance, ^{o}F sq ft hr/Btu.

R_{bfi} — Combined inside fin and bond resistance, ft hr ^{o}F/Btu.

R_f — Fin resistance, ^{o}F sq ft hr/Btu; R_{f1}, of fin Y_1; R_{f3}, of fin Y_3; R_{f2i}, of inside fin Y_2; R_{f2o}, of outside fin Y_2; R_{fi}, of inside fin; R_{fo}, of outside fin.

R_{fO} — Combined outside fin resistance, ft hr ^{o}F/Btu.

R_w — Net radiation from a thermally black, horizontal plane at the wet-bulb air temperature to the sky, Btu/sq ft hr.

s — Slope of a chord on an enthalpy-temperature diagram for air, Btu/^{o}F $lb_{dry\ air}$.

T — Absolute temperature, ^{o}R; T_a, of air; T_s, effective black-body sky temperature.

t Temperature, ^{o}F; t_a, of ambient or outside air; t_e, effective or sol-air temperature; t_{ew}, effective or sol-air temperature for a wet surface; t_f, of fluid; t_{f1}, of entering fluid; t_{f2}, of exiting fluid; $\bar{t}_f$, mean fluid temperature; t_m, of metal surface; t_{mo}, of outside metal; t_{mi}, of inside metal; $\bar{t}_m$, mean metal temperature; t_s, effective sky temperature; t_{wb}, wet-bulb air temperature.

U Overall heat transfer coefficient, Btu/sq ft hr ^{o}F; U_L, overall heat loss coefficient for roof; U_o, overall heat transfer coefficient from the fluid to outside.

W Width of roof, ft.

x_e Equivalent fin length for evaluating fin resistance, ft.

Y Roof section corresponding to a fin length, ft; Y_1, Y_2 and Y_3, outside, bond area, and inside sections, respectively.

α Overall absorptivity of roof for solar radiation.

Δ Difference, or error.

δ Fin thickness, ft.

ϵ Emissivity of roof surface.

ϵ_a Emissivity of atmosphere.

ϵ_w Emissivity of water.

ϵ_x Heat exchanger effectiveness.

ϵ_{xw} Heat exchanger effectiveness of wet roof.

η_f Fin effectiveness.

η_s Solar collector efficiency.

σ Stefan-Boltzmann constant, Btu/(sq ft)(hr)(^oR)^4.

Conversion to SI Units

Btu/lb x 2.326×10^3	J/kg
Btu/lb ^{o}F x 4.187×10^3	J/kgK
Btu/ft hr x 8.933×10^{-2}	J/ms
Btu/sq ft hr x 3.155	J/m^2s
Btu/ft hr ^{o}F x 1.731	J/msK
Btu/sq ft hr ^{o}F x 5.678	J/m^2sK
lb/hr x 1.26×10^{-4}	kg/s
lb/sq ft hr x 1.356×10^{-3}	kg/m^2s
ft x 0.3048	m
sq ft x 9.29×10^{-2}	m^2
(^{o}F - 32) ÷ 1.8	^{o}C
^{o}R ÷ 1.8	K

Residential Cooling by Nocturnal Radiation

ABSTRACT

As part of the U.S. Department of Energy's Passive Cooling program, data were collected from an adobe building in Tucson with a metal roof to evaluate residential cooling by nocturnal radiation. Experimental results were correlated by an equation similar to that used to describe solar collector performance, relating the heat rejection rate ($-q_u$), to the net radiation term (R), the inlet fluid (t_{fl}) and ambient air temperature (t_a), using a plate efficiency factor (F_R) and heat loss coefficient (U_L):

$$-q_u = F_R[\varepsilon R + U_L(t_{fl}-t_a)]$$

Cooling by nocturnal radiation alone was found to be inadequate during peak summer cooling periods. The results were extrapolated to the case of evaporative cooling using a wetted roof; heat rejection from the wet roof appears adequate for residential cooling in a hot, arid climate.

Introduction

During 1981 and 1982 a passive cooling experimental facility for a hot, arid climate was constructed at the Environmental Research Laboratory in Tucson, Arizona as part of the U.S. Department of Energy's Passive Cooling Program. Intended to advance the state of the art of passive and hybrid cooling to a level approaching that of passive solar heating, the facility was designed to test a number of passive cooling strategies appropriate to hot, arid climates in a relatively short time frame. Three test structures and a data aquisition building were constructed, each representing different construction techniques and cooling strategies. One of the test structures, constructed of adobe with a metal roof, was used to evaluate residential cooling by nocturnal radiation.

The effective temperature of a clear night sky is generally lower than the temperature of the air at the earth's surface. This allows a surface, such as a roof, to be cooled at night by radiation to the sky. To cool a building, a fluid such as air is passed through or under the roof at night, cooled, and circulated either through the building to reduce the temperature of the mass of the structure, or through some thermal storage medium, such as a rock bed, which can be used to cool the building during the day.

Water was circulated through the roof of the experimental Solar Energy Laboratory (1) at the University of Arizona in the early 1960's for both nocturnal cooling in summer and solar heating in winter. The water was stored in an insulated, two-compartment tank, and circulated through the ceiling of the building to control its temperature; a heat pump regulated the temperature of the storage tank compartments to assist the solar heating/nocturnal cooling by

the roof. While technically and operationally successful, the Solar Energy Laboratory was not regarded as economically practicable by the designer.

The test structure used in this program consisted of a metal roof containing channels for air circulation, and interior and exterior adobe walls for thermal storage. The building, shown in Figure 1, is fairly typical of southwestern adobe architecture, and incorporates only materials and components readily available to builders, without elaborate controls relative to the interior comfort of the structure. As an experimental structure, it was thoroughly instrumented with sensors to determine the comfort parameters, as well as energy exchange and storage. The radiative cooling function of the building was only one of many of the experimental features, and neither the roof, blower, or internal mass were optimized in the building design; rather, commercially available components and traditional construction techniques were utilized. The roof decking material, for example, was selected as a compromise based on a cursory study of the heat transfer characteristics of commercially available designs.

A thorough study of the building performance will require at least an additional year of data collection; however, the performance of the roof for nocturnal cooling can be characterized based on a limited amount of data, collected in the fall of 1982. Later experimentation with the roof will include evaporative, as well as radiative, cooling, by wetting the roof with a water spray. Since the heat transfer analysis of the dry roof extends naturally to the wet roof case, projections of the performance of a wet roof are included although data has not been collected in this operational mode.

Figure 1. Test structure, east side and roof.

The performance of the roof for nocturnal cooling can be adequately predicted by the approach normally used with flat-plate solar collectors. Cooling of the building by nocturnal radiation appears marginal, at best, while evaporative cooling by a wet roof seems very promising.

Description of Test Structure

The experimental structure, shown in Figures 1 and 2, was built of 16" thick asphalt emulsion stabilized adobe. The structure, similar in plan to a house, was designed based on a low cost solar home originally developed for the Navajo Indians in Northern Arizona. That project was intended to meet the requirements of the U.S. Department of Housing and Urban Development (HUD) while also meeting the needs of the Navajos for a solar heated home. The house was about 1000 square feet with three bedrooms, a bathroom, and a combination living room, dining room and kitchen.

In the test structure, one bedroom was converted to a "family room" adjacent to the living room so an exit could be provided on the north side. Because it was used only for testing, the kitchen and bathroom were only partially installed. The floor plan for the test structure is shown in Figure 3.

The adobe walls and bond beam were nine feet high throughout the structure. The metal roof structural and duct system are attached to the top of the walls creating an average ceiling height of approximately 10'.

The structure contained one interior duct from the solar/screen porch over the kitchen cabinets and into the hallway, as shown in Figure 4. Air

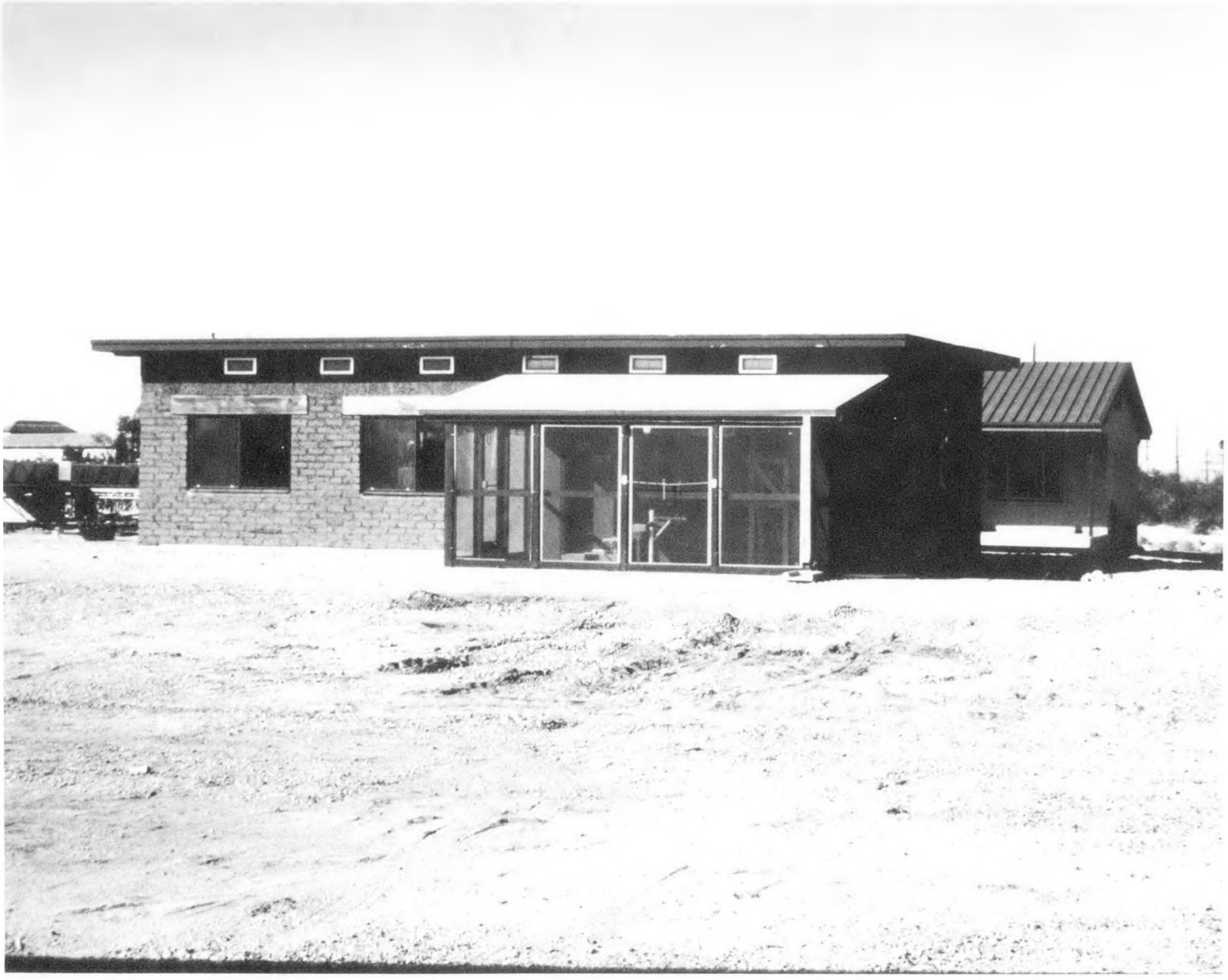

Figure 2. Test structure, south side.

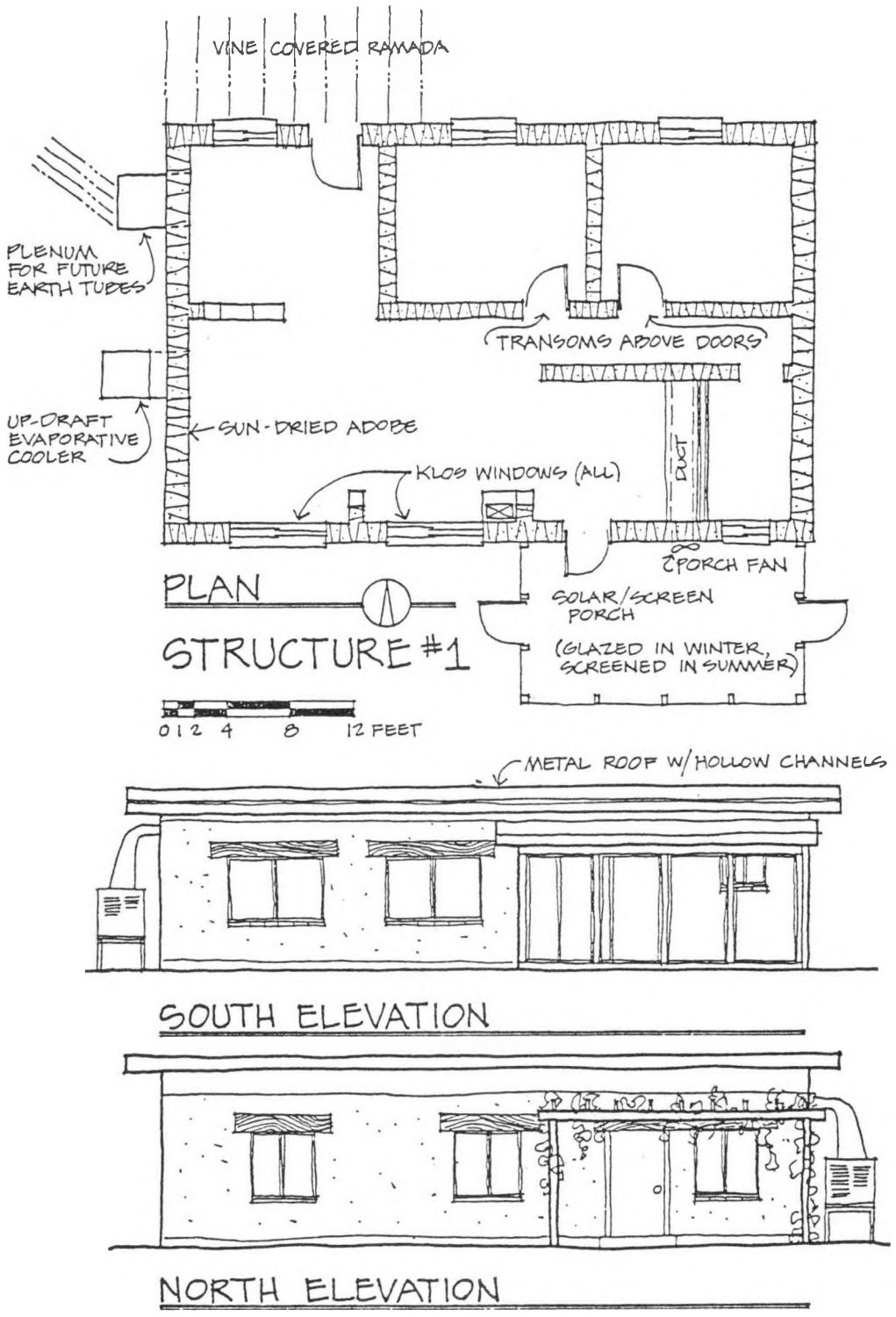

Figure 3. Floor plan.

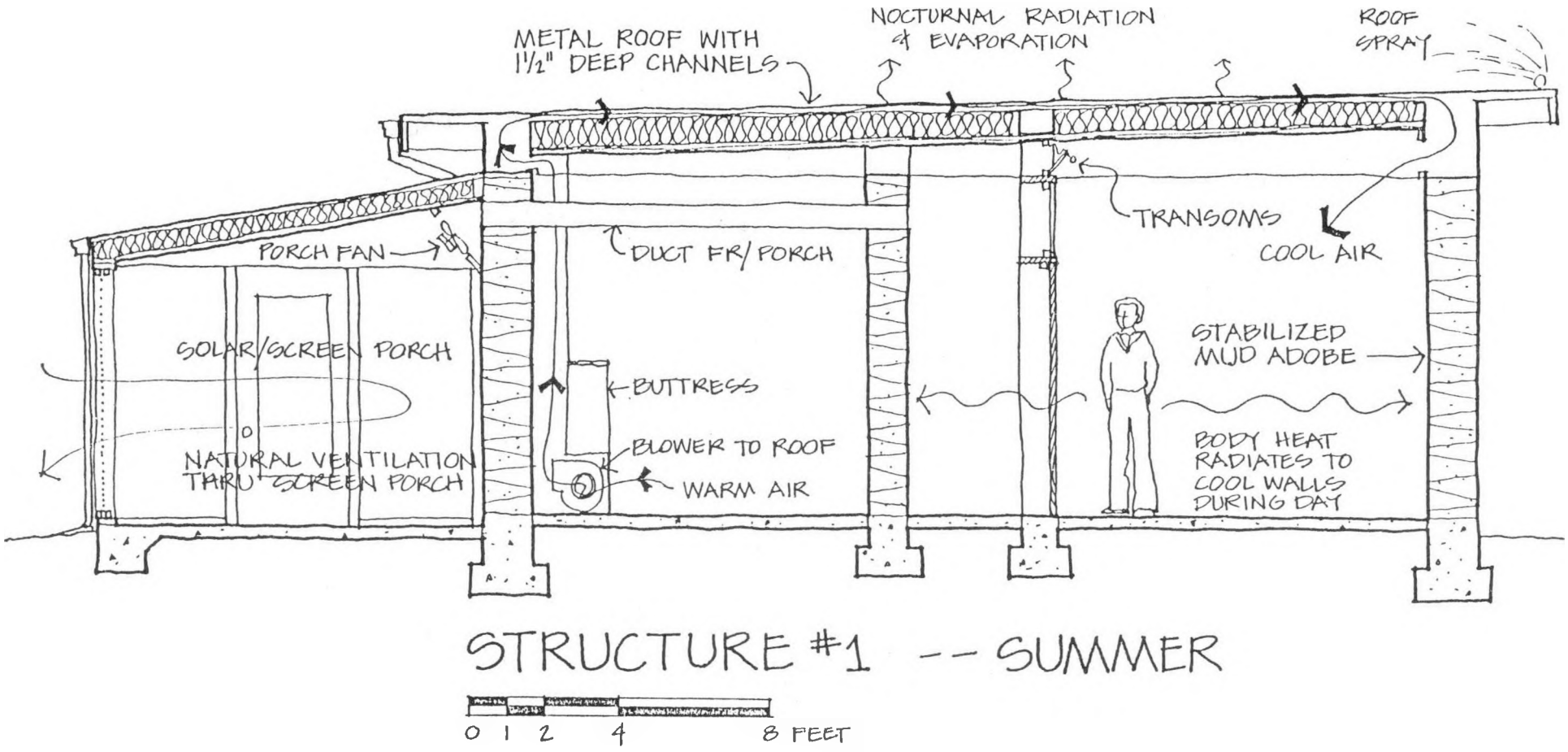

Figure 4. Operation of test structure.

distribution ducts for the roof are located at ceiling height on the north and south sides of the building. Transoms are installed at ceiling height over the central walls.

Passive cooling strategies which may be tested in the structure include nocturnal radiation, evaporation, earth contact, ventilation and the combination of high mass and low mass effects. While only the system for nocturnal radiation will be described here, the building can be modified for wetting the roof to test evaporative cooling using the roof.

For cooling by nocturnal radiation air is blown from inside the structure through channels in the roof and returned to the building interior. As the air passes through the roof, it is cooled by the radiation of heat to the night sky.

Essential to proper air distribution through the roof was a plenum, shown in Figures 5 and 6, which was also used as the major structural support for the roof, and was constructed using galvanized steel formed into a "hat" section. Steel beams and joists attached to the plenum were used to support both the corrugated roof decking and the insulation and ceiling below.

The top of the plenum was bolted to the bond beam running along the top of the adobe wall, and opened onto the bottom of the roof channels.

A flat shed roof using standard steel roof decking (Roll Form Products, Inc., Boston, MA, type RFC 1-1/2, 24", 16/16, G-60, galvanized) shown in Figures 7 and 8 was selected for the roof. It has 1-1/2" deep x approx. 4" wide trapezoidal channels, spaced 6" between centers, through which the air can flow. The size of the channels was selected to provide a velocity giving an interior heat transfer coefficient of 2-3 Btu/(sq ft)(hr)(^{o}F) at a reasonable pressure

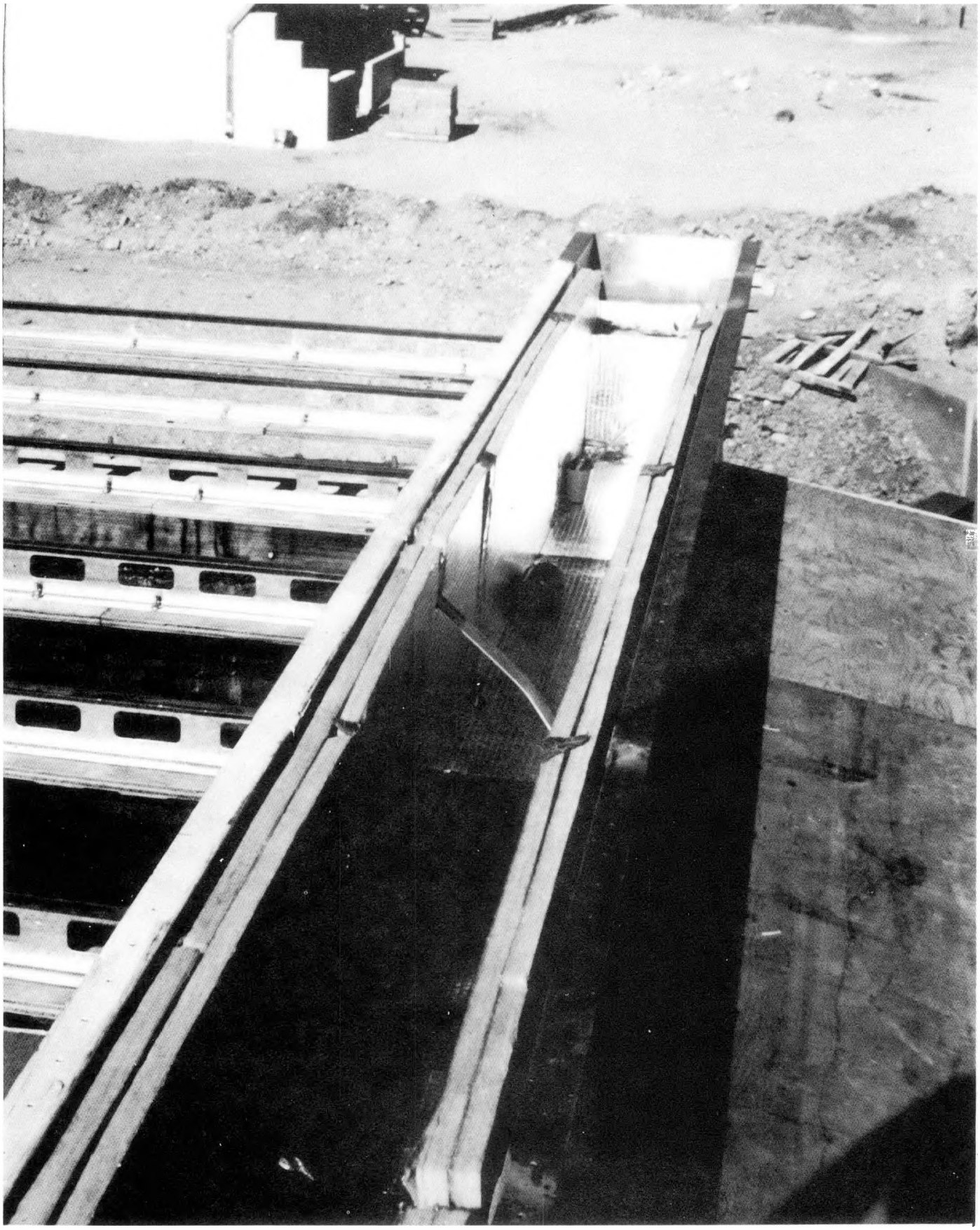

Figure 5. Air distribution plenum, shown during construction.

Figure 6. Air entries from plenum into radiating roof.

Figure 7. Roof decking material, prior to installation.

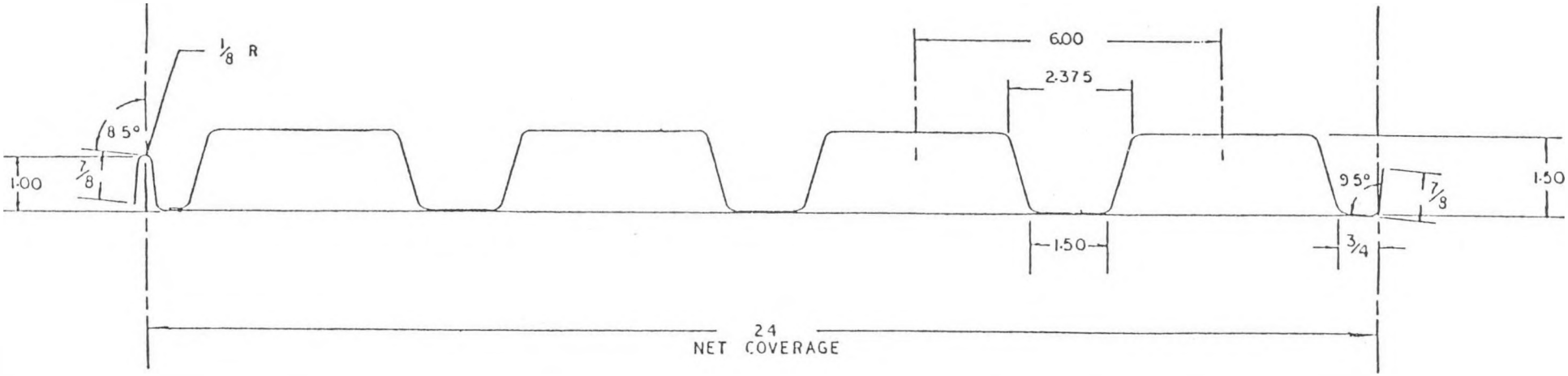

NOTE: Material is 16 gage galvanized steel sheet, spot welded. Installed on roof in an inverted position relative to the above sketch. Dimensions are inches.

Figure 8. Cross-section of experimental roof material.

drop (0.4-0.5 in. water gauge) and blower power requirement.

The steel decking was made with two pieces, one corrugated and the other flat, which are spot welded together. Normally, the corrugated side would face up, but in this case, the flat side was installed facing up to provide a better surface for nocturnal radiation or wetting.

Because the flat side was installed exposed to the weather, waterproofing was somewhat more critical than it would otherwise have been. A high grade polyurethane caulking was used between the panels and the roof was painted white.

A 3" diameter hole was drilled into each corrugation above the plenum to provide for air flow through the roof, as shown in Figure 6. Rectangular openings were cut into both the inside and outside of the metal duct for insertion of aluminum louvers. The louvers are return air grilles ("FRA-FF" louvers) with a 1" space provided for a removable filter, or a 1" board of insulation if the grilles are closed. This makes it possible to either blow air into the structure or exhaust it to the outside. Air is blown through the roof with a 2000 cfm, 1/2 hp blower (Lau Industries, Div. of Philips Industries, Model FOP 15-9CW, Dayton, Ohio).

Below the metal roof, 8" of fiberglass batt insulation was installed and covered with a conventional drywall ceiling.

The roof was relatively expensive to build, costing about $9-10,000 in materials. However, a mass-production scheme could be devised in order to reduce material and labor costs.

Convective and Radiative Cooling

The analysis of a roof for cooling by radiation to the sky at night can be approached in the same manner as a flat-plate solar collector; at night the solar input term becomes zero. Most solar collectors can be described by an equation in the form (1), (2):

$$q_u = F_R[q_A - \varepsilon R - U_L(t_{fl} - t_a)] \qquad (1)$$

where q_u is the average useful heat collection rate, Btu/(sq ft)(hr); F_R is the collector plate efficiency factor; q_A is the total solar radiation absorption rate; ε is the average emissivity of the surface for long-wave radiation; R is the net radiation from a thermally black horizontal plane at air temperature to the sky, Btu/(sq ft)(hr); U_L is the overall heat loss coefficient for the collector, Btu/(sq ft)(hr)(^oF); t_{fl} is the temperature of fluid entering the collector, ^oF; and t_a is the outdoor air temperature.

If $q_A = \alpha q_s$, where α is the overall absorptivity of the collector plate for solar radiation, and q_s is the total incident solar radiation on the collector, the efficiency of the collector (η_s) for solar energy collection is generally written:

$$\eta_s = q_u/q_s = F_R\{\alpha - [\varepsilon R + U_L(t_{fl} - t_a)]/q_s\} \qquad (2)$$

and correlations are often obtained by plotting η_s vs. $(t_{fl} - t_a)/q_s$, with $\varepsilon R/q_s$ often assumed to be negligible. Since $\varepsilon R/q_s$ is generally one-tenth or less of η_s, this is usually regarded as acceptable for most applications. In this application, the primary concern is the long-wave

diation term R, with $q_A = 0$, in which case an efficiency term relating to e heat rejection rate from the collector (radiator) can be used to advantage:

$$q_u/_R = - F_R[\varepsilon + U_L(t_{fl} - t_a)/R] \quad (3)$$

$- q_u/R$ can be expected to yield a straight line when plotted against $_{fl} - t_a)/R$, with an intercept of $F_R\varepsilon$ and a slope of F_RU_L.

Expressions for the terms in equations 1 - 3 can be derived for simple roof metries in a straightforward manner using the "sol-air" temperature approach scribed in the ASHRAE handbook (3), where the sol-air temperature, t_e is fined as:

$$t_e = [(q_A - \varepsilon R)/h_o] + t_a \quad (4)$$

re h_o is the combined convective and radiative heat transfer coefficient $_o + \varepsilon h_r$), between the roof, or metal (t_m), surface and the ambient air sky (3). For example, if t_s is the effective black-body sky temperature, al to $(A/\sigma)^{1/4} - 460$, ^oF, where A is the intensity of atmospheric iation, Btu/(sq ft)(hr), sometimes written as $\varepsilon_a\sigma T_a^4$, with T_a the olute air temperature, ^oR, ε_a the emissivity of the atmosphere, and σ the fan-Boltzmann constant, Btu/(sq ft)(hr)$(^oR)^4$; then t_e can be deduced m a balance around the surface, as:

$$q_A + h_{co}(t_a - t_m) + \varepsilon h_r(t_s - t_m) = (h_{co} + \varepsilon h_r)(t_e - t_m) \quad (5)$$

since $R = h_r(t_a - t_s)$

$$t_e = (q_A + h_{co}t_a + \varepsilon h_r t_s)/(h_{co} + \varepsilon h_r)$$

$$= [(q_A - \varepsilon R)/h_o] + t_a \qquad (4)$$

Using the sol-air temperature, t_e, and U_o, the overall heat transfer coefficient from the fluid to the outside, Btu/(sq ft)(hr)(^oF), then a heat balance around a differential element of length, dL, is given by:

$$m_f c_{pf} dt_f/dL = U_o W(t_e - t_f) \qquad (6)$$

where W is the width of roof, ft. This assumes that the heat flow downward from the roof into the house can be neglected. Equation 6 can be integrated to give

$$\ln[(t_{f2} - t_e)/(t_{f1} - t_e)] = - U_o WL/m_f c_{pf} \qquad (7)$$

note that $WL = A_f$, the area of the roof under which the fluid is flowing, sq ft, and $m_f/A_f = G$, lb/(sq ft) (hr). The number of transfer units for the roof, N_t, when viewed as a heat exchanger is:

$$N_t = U_o/Gc_{pf} \qquad (8)$$

and the heat exchanger effectiveness ε_x (4), of the roof is:

$$\varepsilon_x = (t_{f2} - t_{f1})/(t_e - t_{f1}) = 1 - EXP(-N_t) \qquad (9)$$

which agrees with textbook definitions for ε_x if the atmosphere is viewed as a fluid stream of infinite heat capacity (4). Also, the integrated average fluid temperature along the roof can be found as:

$$\bar{t}_f = t_{f1} + (t_{f2} - t_{f1})[(1/\varepsilon_x) - (1/N_t)] \tag{10}$$

$\bar{t}_f$ is used in computing the average outside roof temperature, $\bar{t}_m$, which is required to determine the outside radiative coefficient, h_r.

$$\bar{t}_m = (U_o/h_o)(\bar{t}_f - t_e) + t_e \tag{11}$$

Determination of $\bar{t}_m$ and h_r is an iterative process. The average heat collection rate, q_u, is from equation 9;

$$\begin{aligned} q_u &= Gc_{pf}(t_{f2} - t_{f1}) = Gc_{pf}\varepsilon_x(t_e - t_{f1}) \\ &= Gc_{pf}\varepsilon_x \{[(q_A - \varepsilon R)/h_o] + t_a - t_{f1}\} \\ &= (U_o/h_o)\ (Gc_{pf}/U_o)\ [1 - EXP(-N_t)]\{q_A - \varepsilon R - h_o(t_{f1} - t_a)\} \end{aligned}$$

$$q_u = (U_o/h_o)(1/N_t)[1 - EXP(-N_t)]\{q_A - \varepsilon R - h_o(t_{f1} - t_a)\} \tag{12}$$

Comparing this with equation 1

$$F_R = (U_o/h_o)(1/N_t)[1 - EXP(-N_t)] \tag{13}$$

and $U_L = h_o = h_{co} + \epsilon h_r$ (14)

Evaporative and Radiative Cooling

In many dry locations where nocturnal radiation can be used for cooling, evaporative cooling provided by a film of water on the roof can also be used to some advantage.

The sol-air temperature method, modified to allow for evaporation from the surface, is again useful. An energy balance at the wet metal surface is given by:

$$q_A + h_{co}(t_a - t_m) + k_{co}\,\lambda\,(H_a - H_m) + \epsilon_w h_r(t_s - t_m) = h_{ow}(t_{ew} - t_m) \quad (15)$$

where k_{co} is the mass transfer coefficient, lb/(sq. ft.)(hr)(unit ΔH); λ is the heat of vaporization of water, Btu/lb; H_a is the humidity of the outside air, lb_{water}/lb_{air}; and H_m is the humidity of air at the water surface, or the humidity of saturated air at t_m; ϵ_w is the emissivity of water; h_{ow} is the combined heat transfer coefficient at the wet outside surface, and t_{ew} is the sol-air temperature for a wet surface, ^oF. The Lewis relation (3), commonly used in cooling tower analysis, is often written:

$$k_{co} = h_{co}/c_s \quad (16)$$

where c_s is the specific heat of moist air, Btu/(lb air)(^oF).

The convective mass and heat transfer terms in equation 15 can be written:

$$h_{co}(t_a - t_m) + k_{co}\lambda(H_a - H_m) = (c_s k_{co})(t_a - t_m) + k_{co}\lambda(H_a - H_m) \qquad (17)$$

while the enthalpy difference between the ambient air and air at the wet interface is

$$i_a - i_m = c_s(t_a - t_m) + \lambda(H_a - H_m) \qquad (18)$$

where i is enthalpy, Btu/lb air

then: $$h_{co}(t_a - t_m) + k_{co}\lambda(H_a - H_m) = k_{co}(i_a - i_m) \qquad (19)$$

At a given wet-bulb air temperature, the enthalpy can be considered approximately constant. If $s = (i_a - i_m)/(t_{wb} - t_m)$, $(\cong di/dt)$, where s is the slope of a chord on an enthalpy-temperature diagram for air, then equation 17 becomes

$$h_{co}(t_a - t_m) + k_{co}\lambda(H_a - H_m) = (h_{co}s/c_s)(t_{wb} - t_m) \qquad (20)$$

where t_{wb} is the wet-bulb temperature of the ambient air, ^{o}F.

Equation 15 can now be written as:

$$q_A + h_{co}(t_a - t_m) + k_{co}\lambda(H_a - H_m) + \varepsilon_w h_r(t_s - t_m) =$$
$$q_A + (h_{co}\, s/c_s)(t_{wb} - t_m) + \varepsilon_w h_r(t_s - t_m) =$$
$$q_A + [(h_{co}s/c_s) + \varepsilon_w h_r](t_{wb} - t_m) - \varepsilon_w h_r(t_{wb} - t_s) \qquad (21)$$

If $R_w = h_r(t_{wb} - t_s)$, the net radiation from a thermally black horizontal plane at the wet-bulb air temperature to the sky, then

$$[(h_{co}s/c_s) + \varepsilon_w h_r]\ \{(q_A - \varepsilon_w R_w)/[(h_{co}s/c_s) + \varepsilon_w h_r] + t_{wb} - t_m\} =$$
$$h_{ow}(t_{ew} - t_m) \qquad (22)$$

Then the sol-air temperature for a wet surface is:

$$t_{ew} = \{(q_A - \varepsilon_w R_w)/[(h_{co}s/c_s) + \varepsilon_w h_r]\} + t_{wb} \qquad (23)$$

with the combined outside heat transfer coefficient given by:

$$h_{ow} = [(h_{co}s/c_s) + \varepsilon_w h_r] \qquad (24)$$

Derivation of the overall performance equation for a wet roof parallels that of the dry roof, with t_{ew} replacing t_e, h_{ow} replacing h_o, t_{wb} replacing t_a, and $\varepsilon_w R_w$ replacing εR. The heat exchanger effectiveness for the wet roof is given by

$$\varepsilon_{xw} = (t_{f2} - t_{f1})/(t_{ew} - t_{f1}) = 1-EXP(-N_{tw}) \quad (25)$$

where U_o in N_{tw} is evaluated with h_{ow} replacing h_o. Note that if $q_A - \varepsilon_w R_w = 0$, $t_{ew} = t_{wb}$, then ε_{xw} becomes the evaporative cooler effectiveness (5), with the moisture content of the fluid stream unchanged.

For the wet roof, the overall performance equation corresponding to equation 1 for the dry roof becomes:

$$q_{uw} = F_{Rw}[q_A - \varepsilon_w R_w - h_{ow}(t_{f1} - t_{wb})] \quad (26)$$

where h_{ow} is given by equation (24) and F_{Rw} by

$$F_{Rw} = (U_{ow}/h_{ow})(1/N_{tw})[1 - EXP(-N_{tw})] \quad (27)$$

In comparing the wet roof with the dry roof, $t_{f1} - t_{wb}$ is usually greater than $t_{f1} - t_a$, h_{ow} is larger than h_o; however, $\varepsilon_w R_w$ is less than εR; the net results are generally that a wet roof can reject heat considerably more effectively than a dry roof.

One word of caution in using the expressions for a wet roof: the s term in h_{ow} changes rapidly with temperature, and $\bar{t}_m$ must be evaluated carefully to determine s, from:

$$\bar{t}_m = (U_{ow}/h_{ow})(\bar{t}_f - t_{ew}) + t_{ew} \quad (28)$$

The use of enthalpy for treating combined heat and mass transfer from the roof can result in minor errors. The use of a "transfer function" as described in the literature (8) is more accurate, but is rarely used. Considering the many years of engineering design experience with the use of the enthalpy potential in cooling tower design, its use is justified here.

Non-linearity of the enthalpy-temperature curve can also result in small inaccuracies when the equations presented here are used. However, in the temperature range normally encountered in residential cooling, the error will normally not exceed 5%.

Overall Heat Transfer Coefficient

Equations 1 - 28 apply to flat, horizontal roofs regardless of the fluid used, whether air or water, or the internal construction, whether tubes or air ducts. In determining the overall heat transfer coefficient, U_o, from the fluid to the outside, the construction of the experimental roof, shown in Figure 8, must be considered, and the heat transfer coefficients must be evaluated for air flowing in the channels.

Referring to Figure 8, the fluid being cooled by nocturnal radiation (air) flows in the closed trapezoidal sections, with the flat surface of the roof decking exposed to the night sky. The interior convective coefficient can be evaluated without difficulty, using the hydraulic diameter of the trapezoidal channel = 4 x cross-section area ÷ perimeter, here ~ 2.2", and widely available heat transfer correlations in the literature (4), (14).

Considerably more uncertainty is involved in the evaluation of the convective heat transfer coefficient at the outside surface of the roof. In this work, the equation used was $h_{co} = 0.7 + 0.28V_w$, for air flow over smooth surfaces (6), where V_w is the wind velocity, miles/hr. In these experiments the wind velocity was measured upstream, and on the plane, of the roof. Recent correlations (7), considering the effect of orientation and eaves on the heat transfer coefficient, do not extend to the large Reynold's numbers encountered here.

The roof section shown in Figure 8 consists of two sheets of 16 gage galvanized steel, spot welded. Referring to Figure 9, appreciable bond resistance to heat transfer can be expected in the area designated Y_2, complicated by the presence of two sheets of metal which are essentially fins. For analytical purposes, one-half of a flow channel can be considered to be composed of four "fins." When fins extend from wall to wall, the effective fin length is half the wall spacing (4), hence the choice of one-half of a channel for analysis. The four fins consist of Y_1, exchanging heat with the internal air stream and the bond area while being insulated underneath; Y_3 exchanging heat with both the internal air stream, the outside atmosphere, as well as the bond area; and the upper and lower Y_2 sections, sandwiching the bond.

The effectiveness of thin sheet fins of constant conduction cross-section is given by (4):

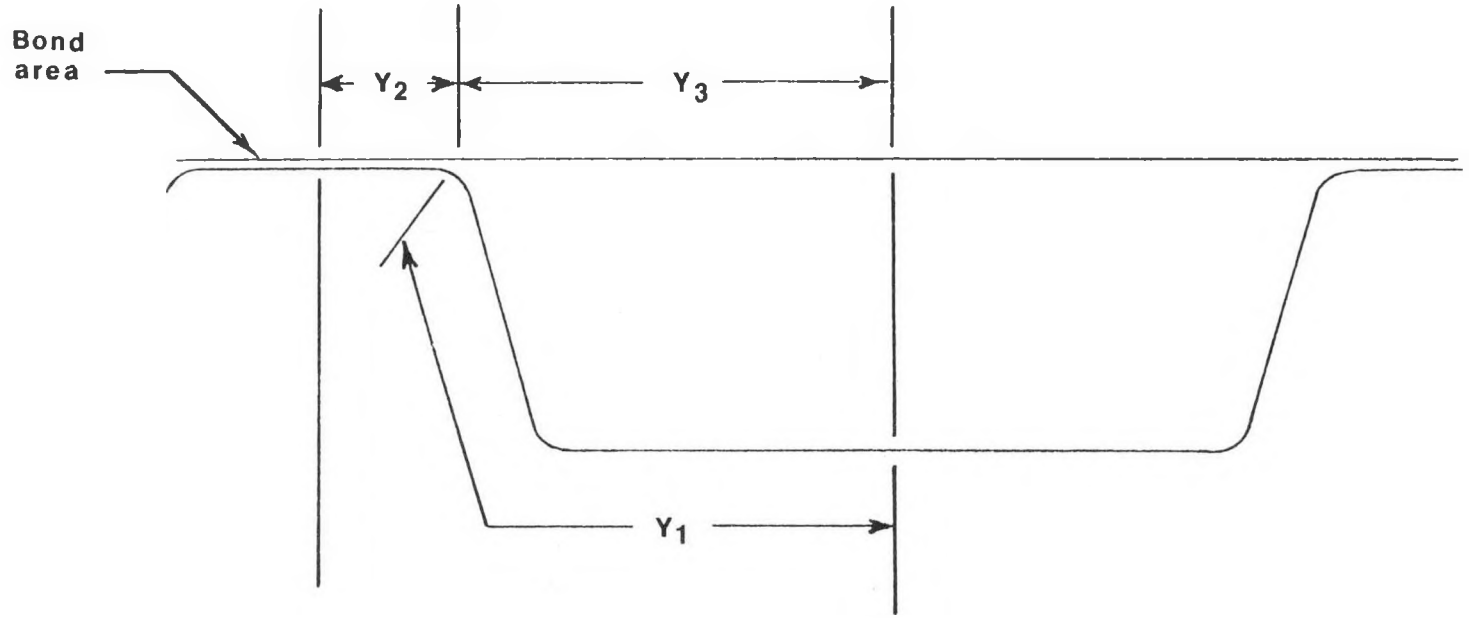

Figure 9. Cross-section of roof channel showing equivalent fin sections.

$$\eta_f = (\tanh m\ell)/m\ell \tag{29}$$

$$\text{where } m = \sqrt{2h/k_m \delta} \tag{30}$$

when heat transfer occurs on both sides of the fin with the convective coefficient on both sides equal to h. δ is the fin thickness, ft., ℓ is the fin length, ft., and k_m is the thermal conductivity of the metal fin, Btu/ft hr ^oF. If heat transfer occurs only one side of the fin; e.g., section Y_1, Figure 9, then $m = \sqrt{h/k_m \delta}$. With the air flow rates included in this work, η_f for Y_1 was in the range 0.69 to 0.77, so the fin effectiveness cannot be neglected.

The fin effectiveness term is difficult to apply to section Y_2 because of the bond resistance; to avoid a lengthy analytical or finite difference solution of this geometry, the fin resistance can be used instead of the fin effectiveness. Consider a fin of unit width, insulated on one side; heat transfer into the base of the fin using the fin effectiveness is

$$Q = h\ell\eta_f\Delta t \tag{31}$$

where Δt is the temperature difference between the fluid surrounding the fin and the base of the fin.

Using the fin resistance (R_f), expression 31 becomes

$$Q = [1/(R_f/\delta) + (1/h\ell)]\Delta t \tag{32}$$

where $R_f = x_e/k_m$. By algebraic manipulation of equations 29–32 it may be demonstrated that

$$x_e/\ell = (1/m\ell)^2[(m\ell/\tanh m\ell) - 1] \tag{33}$$

as shown in Table I, x_e/ℓ is fairly stable for low values of $m\ell$, with $x_e/\ell \sim 1/3$.

Table I

Equivalent Fin Length for Evaluating Fin Resistance

$m\ell$	x_e/ℓ
0.1	1/3
0.4	0.33
0.8	0.32
1.0	0.31
1.5	0.29

In this work, $m\ell$ for the fins in section Y_2 was less than 0.8, hence $x_e/\ell \sim 1/3$ is a good approximation, for the longer fin Y_1, $m\ell$ was as high as 1.2, giving $x_e/\ell = 0.3$, which would give about a 10% error if $x_e/\ell = 1/3$ was assumed. In the case of sections Y_1 and Y_3 the heat transfer coefficients are known, so either the fin resistance or fin effectiveness can be used; to be consistent, the fin resistance term is used in the equations which follow.

For the composite fin in section Y_2, if R_{fo} is the fin resistance of

the outer fin, and R_{fi} the resistance of the inner fin, in this instance both values of R_f are approximately $(1/3)(Y_2/k_m)$. If t_{mo} is the temperature at the base of the outer fin, where Y_2 joins Y_3, and t_{mi} the temperature of the base of the inner fin, where Y_2 joins Y_1, then the heat flow from the top of the bond section Y_2 is:

$$Q = \frac{h_o Y_2 \left\{(\delta/R_{fo})(t_{mo} - t_e) + \{1/[(R_{fi}/\delta) + (R_b/Y_2)]\}(t_{mi} - t_e)\right\}}{(\delta/R_{fo}) + \{1/[(R_{fi}/\delta) + (R_b/Y_2)]\} + h_o Y_2} \qquad (34)$$

where R_b is the bond resistance between the two metal sheets, $ft^2 hr\,^oF/Btu$. From experimental data, the bond resistance was found to be approximately 0.08 $(ft^2)(hr)(^oF)/Btu$. To appreciate the relative influences of the temperatures of the fin bases, equation 34 evaluated for the dry roof is:

$$Q = h_o Y_2[0.89(t_{mo} - t_e) + 0.09(t_{mi} - t_e)] \qquad (34)$$

If $t_{mo} = t_{mi}$; $Q = h_o Y_2[0.98(t_m - t_e)]$; the usual fin effectiveness approach gives $\eta_f = 0.977$ for 1δ and $\eta_f = 0.98$ for 2δ.

Now, if R_{f1} is resistance of the fin Y_1, R_{f3} the resistance of the section Y_3, R_{f2i} the resistance of the inner fin for section Y_2, and R_{f2o} the resistance for the outer fin of Y_2, let

$$(R_b/Y_2) + (R_{f2i}/\delta) + (R_{f1}/\delta) = R_{bfi} \qquad (35)$$

and $(R_{f2o}/\delta) + (R_{f3}/\delta) = R_{fO}$

then the overall coefficient, based on the outside area $Y_2 + Y_3$ is:

$$U_o = \frac{1}{(Y_2 + Y_3)} \left\{ \left[\frac{1}{R_{bfi} + (1/h_{ci}Y_3)} \right] \left\{ \frac{h_o Y_2 + \dfrac{h_o Y_3}{[R_{fo}Y_3(h_o + h_{ci}) + 1]}}{\left(\dfrac{1}{R_{bfi} + (1/h_{ci}Y_3)} + h_o Y_2 \right) + \dfrac{Y_3(h_o + h_{ci})}{[R_{fo}Y_3(h_o + h_{ci}) + 1]}} \right\} \right.$$

$$\left. + h_{ci}Y_3 \left\{ \frac{h_o Y_3 + \dfrac{h_o Y_2}{\left[R_{fo} \left(\dfrac{1}{R_{bfi} + (1/h_{ci}Y_3)} + h_o Y_2 \right) + 1 \right]}}{Y_3(h_o + h_{ci}) + \left[\dfrac{\dfrac{1}{R_{bfi} + (1/h_{ci}Y_3)} + h_o Y_2}{R_{fo} \left(\dfrac{1}{R_{bfi} + (1/h_{ci}Y_3)} + h_o Y_2 \right) + 1} \right]} \right\} \right\} \qquad (36)$$

This expression is simplified if it is assumed that there is no heat transfer from the section Y_3 into the bond area Y_2, i.e. $R_{fO} \to \infty$, then, with an error of 1 to 3%:

$$U_o = \frac{1}{(Y_2 + Y_3)} \left[\frac{1}{R_{bfi} + (1/h_{ci}Y_1) + (1/h_oY_2)} + \frac{Y_3}{(1/h_o) + (1/h_{ci})} \right] \qquad (37)$$

Results

Collection of data from the roof began in April 1982, however, the building was not operated in an experimental mode compatable with nocturnal cooling until late summer, and clear-sky data analysis from the roof has been restricted to September 18 and 19, 1982 for the design air-flow throughout the roof, nominally 2000 CFM, and October 9-12, 1982 for a reduced low-speed air flow of approximately 1400 CFM.

More desirable would have been collection of data during the entire cooling season with a suitable cooling load in the building; hopefully, such experiments can be performed in the future.

From the outset of the program, there was some confidence that the performance of the roof could be predicted from past experiments (1) and conventional heat transfer correlations in the literature. Based on experience with other programs involving humidification and dehumidification of air (8), the results of these experiments were extrapolated to the case of a wetted roof. The wetted roof presents special problems in practice involving water

distribution, recirculation, scaling and corrosion, which must be addressed in some future program; however, because of its obvious attractiveness in a desert climate, the calculated heat rejection rates from a wet roof are presented here, along with the dry roof correlations and data.

Raw data including atmospheric (long-wave) radiation, dry and wet bulb ambient temperatures, air temperatures associated with the roof, and wind velocity and direction are presented in Appendix I.

Temperatures were measured with copper-constantan thermocouples, atmospheric radiation with a pyrgeometer (9), and wind velocity with a Gill propeller vane (10) anemometer. The data were collected every ten minutes, and averaged for hourly values. A serious defect of the data collection system was the wind velocity measurement, which averaged 6 instantaneous values each hour to give a single average value for wind velocity. Since wind velocity can vary widely and erratically, such a measurement is a poor indication of the true average. A device giving an integrated average velocity would have been much better. The poor wind velocity measurements undoubtedly contributed to scatter in the experimental correlations.

With regard to atmospheric radiation, a recent paper by Berdahl and Fromberg (11) describes in detail the theory and history of such measurements. When the measurements of Appendix I for clear night skies were converted to emissivity values, experimental values agreed with Berdahl and Fromberg's equation (ε_a = 0.754 + 0.058 x dew point temperature, ^{o}C) using their standard error of estimate (0.033) at a 95% confidence level. Dr. Sellers' equation (12) ($\varepsilon_a = 0.605 + 0.048\sqrt{\text{vap. press } H_2O, \text{mb}}$) was nearer the

experimental values for the September 18-19 data, with Berdahl and Frombergs' values being high by $\cong$ 0.03 as shown in Figure 10. In the October 9-12 data, Sellers', and Berdahl and Frombergs' equations gave essentially the same results, being slightly high by 0.01. Berdahl and Frombergs' paper further presents the correlations of other investigators, in addition to their own and Dr. Sellers'. Hence, it may be possible to obtain fairly good estimates of clear sky atmospheric radiation from weather bureau data in the absence of experimental pyrgeometer data.

It should be mentioned that a seemingly small error in ε_a can result in a surprising large error in the net radiation term R. Since $R = (1 - \varepsilon_a)\sigma T_a^4$, if the error in ε_a is $\Delta\varepsilon_a$, the percent error in R is $100 \times \Delta\varepsilon_a/(1 - \varepsilon_a)$. For example, if $\varepsilon_a = 0.8$ and $\Delta\varepsilon_a = 0.02$ the error is 10%.

In the experimental house, air was blown from the interior into a distribution duct, through 88 three inch diameter holes into the roof decking channel, through the roof, and returned to the house through 3" exit holes, a second distribution duct, and return air grilles. The 1/2 hp blower (13) used for air circulation was nominally rated at 2000 CFM; the blower was equipped with a two-speed motor and provided approximately 1400 CFM at its lower speed. Actual flow rates were measured with a Pitot tube using the ASHRAE traverse method (3) and were determined to be 2090 CFM (8580 lb/hr) and 1390 CFM (5740 lb/hr). Corresponding velocities in the roof channels were 560 and 370 FPM, which produced interior, air-side heat transfer coefficients of 2.8 and 1.8 Btu/(sq ft)(hr)(^{o}F) when computed using heat transfer correlations in the literature (14).

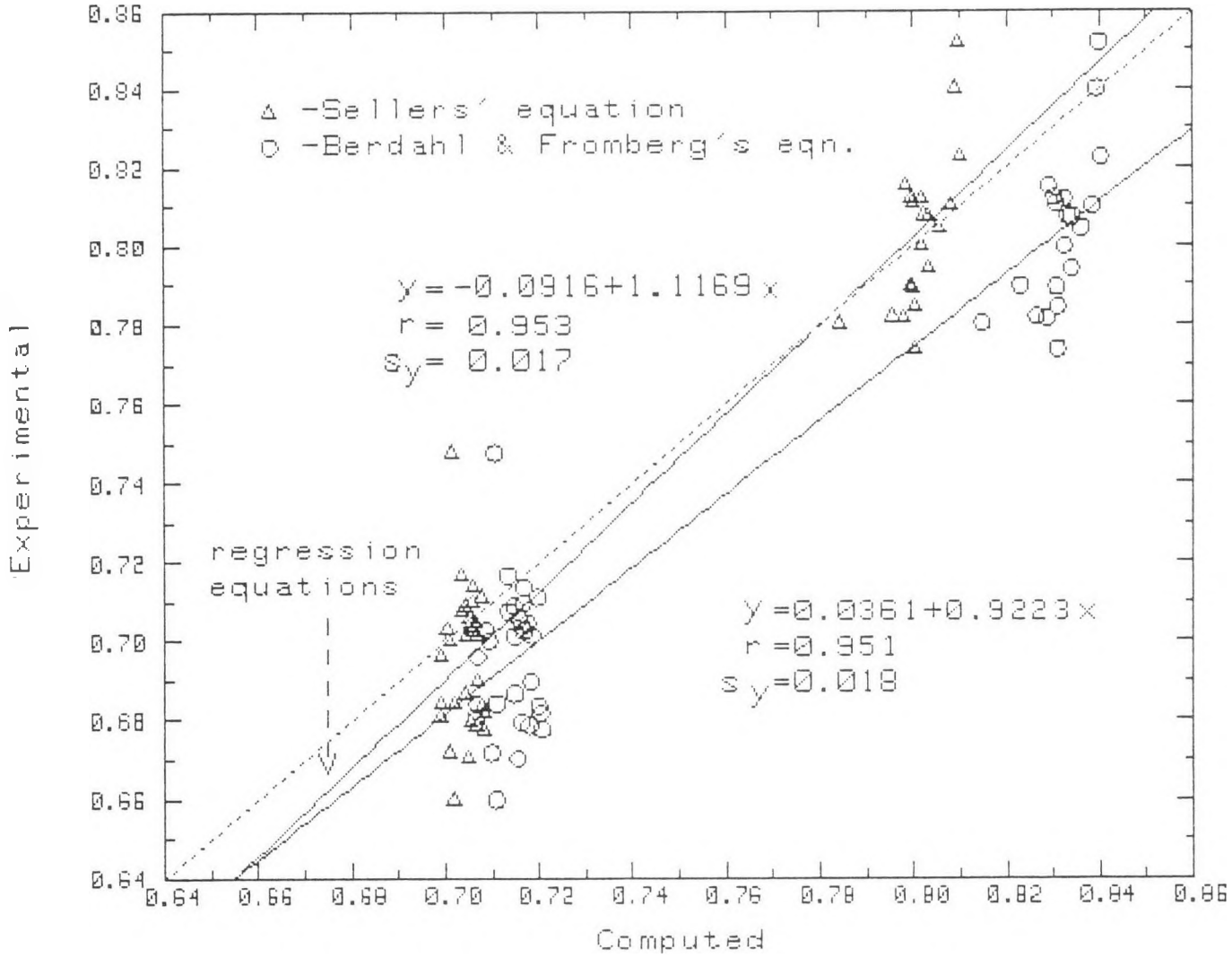

Figure 10. Comparison of computed and experimental sky emissivities.

Air temperatures were measured at the channel inlets and outlet grilles at the east, middle, and west portions of the roof, to obtain the heat rejection rates.

Measurements of the air velocities at the seven outlet grilles indicated some maldistribution of air flow through the roof, as shown in Table II. The center portion of the roof has the greatest air velocity through it, approximately 16% above average. The west air flow measurement (grille no. 2) was nearly equal to the true average, and temperature measurements associated with this section were used to calculate the heat rejection rate, and for other correlations of the data. Graphs based on the arithmetic average and a weighted average of temperatures are also presented in Appendix II.

Table II

Distribution of air flow through outlet grilles

Grille No.	Percent of total air flow
1	14.07
2	14.24
3	13.90
4	16.64
5	12.06
6	14.13
7	14.96

Note: Grilles are equally spaced at 5.7', numbered from the west. Outlet thermocouples were located at grilles 2 (west), 4 (center), and 6 (east). The ideal average flow should be 100/7 = 14.29%.

The roof design of the experimental house had eaves overhanging the north and south ends; the total N-S length of the roof was 30-2/3', while the length of the air-flow channel was 25-1/3 ft, giving an effective "active" area of 83% of the total roof area. The total roof area was used as a basis for all computations, so all analytical values of heat rejection rates computed from the equations presented earlier are multiplied by 0.83. Conduction from the inactive roof area (eaves) to the active area was considered by treating these areas as large fins; offsetting this was the masking of the roof areas where thick polyurethane caulking was used to waterproof joints in the roof decking. These effects roughly cancelled each other, so that a constant value of 0.83 was used for the roof area ratio.

Figure 11 is a plot of $- q_u/R$ vs $(t_{f1} - t_a)/R$ for the night data from the test periods, where $q_u = m_f c_{pf} (t_{f2} - t_{f1})/A_r$, with A_r the total roof area. The solid lines are the results of analytical computations based on the average conditions during the test periods. The emissivity of the roof was taken as 0.95 (15), typical for the white paint used for the roof. Computed values for the overall heat transfer coefficients and the collector efficiency factors were: $U_o = 1.4$, $F_R = 0.40$ at the higher air flow rate and $U_o = 1.2$, $F_R = 0.33$, at the lower air flow. As previously explained, only 83% of the roof was "active". The heat exchanger effectiveness of the roof for the two air flows was 0.54 at the higher air flow and 0.62 at the lower flow.

An alternate method of correlating the roof data would be to plot $(t_{f1} - t_{f2})/(t_a - t_s)$ against $(t_{f1} - t_a)/(t_a - t_s)$, where t_s

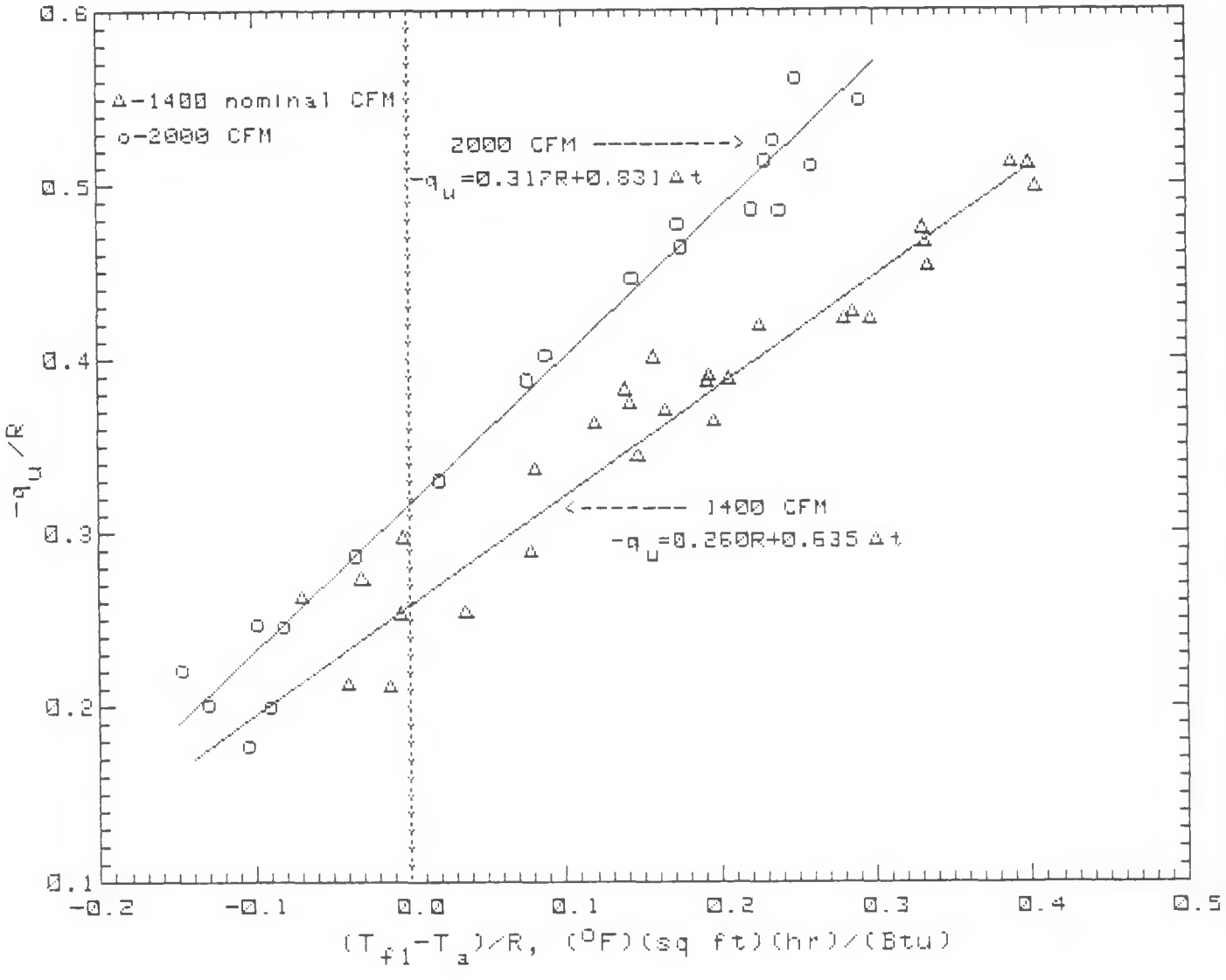

Figure 11. Correlation of experimental data.

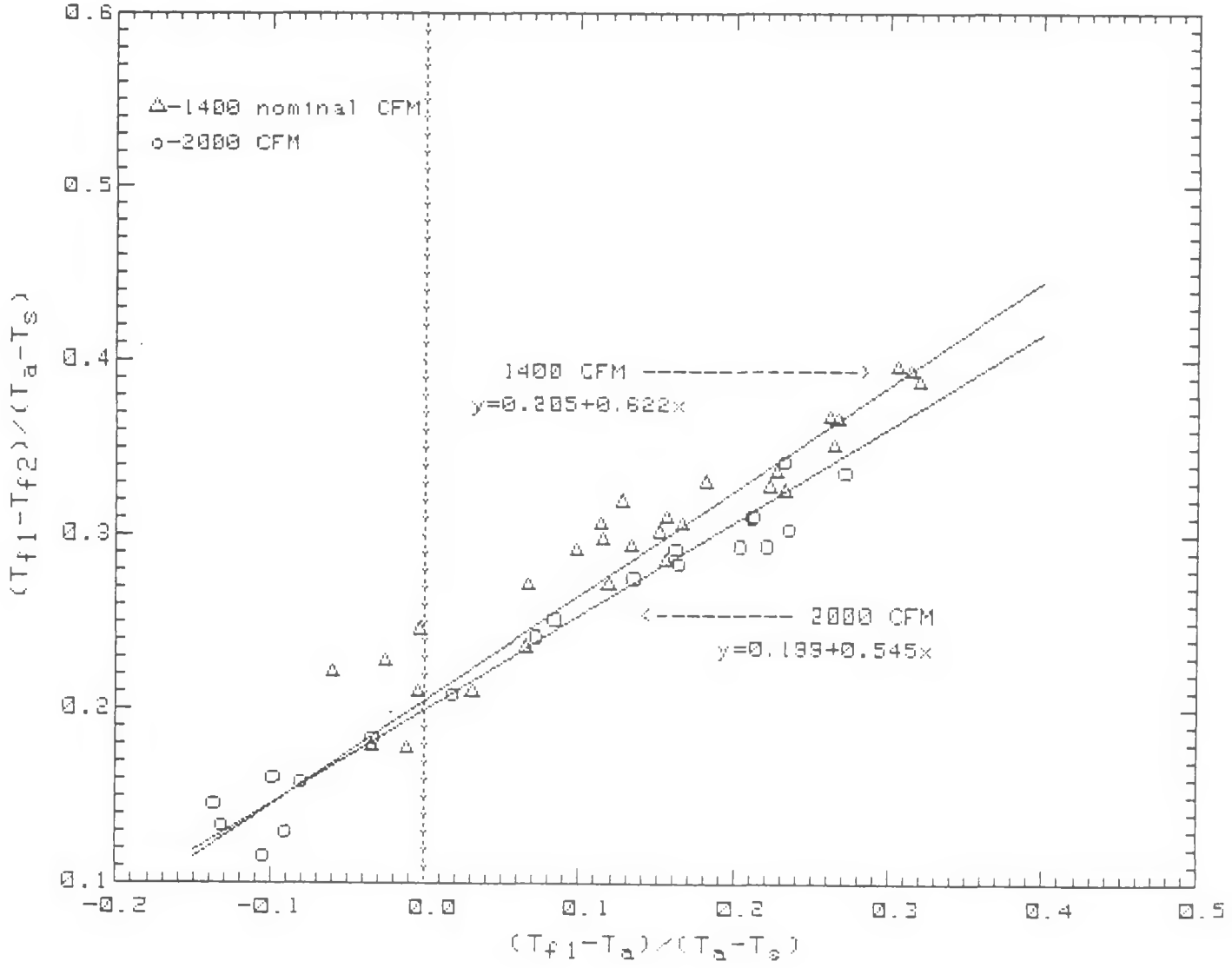

Figure 12. Alternate correlation of experimental data.

is the effective black body sky temperature, from an algebraic rearrangement of equation 9. Results of this type of analysis are shown in Figure 12. The scatter in Figure 12 is probably due to fluctuations in h_{co}, which is strongly influenced by wind velocity and direction, as well as gusts of wind.

Figure 13 is a plot of experimental values of q_u against computed values; where averaged values of wind velocity and temperature dependent parameters were used to compute the lines in Figure 11, actual measured values for each point were used in preparing Figure 13. Computed values of q_u appear slightly high at the higher values for q_u, and low on the low end of the scale. The values of the heat rejection rate are not particularly impressive, less than 20 Btu/(sq ft)(hr); however, the data were not collected during the maximum cooling period, and there was no cooling load in the building to provide a high temperature difference for heat rejection. To completely characterize the performance of the test roof over a range of air flow rates, Tables III-VI were prepared, giving U_o and F_R as functions of air flow and outside heat transfer coefficients.

Figure 14 shows the computed values for roof performance under average conditions for Tucson during June of 1982 (16) and for the 1% ASHRAE summer design conditions (3), for both the dry and wet roof. An adobe building of similar design would require approximately 0.9 tons of refrigerative air conditioning under the ASHRAE conditions; the dry roof alone is clearly inadequate to maintain comfortable conditions under the ASHRAE conditions, and marginal under average June conditions. Figure 14 was prepared using a solar absorptivity for the white roof of $\alpha = 0.25$, corresponding to a slightly soiled

experimental roof. In the case of the wetted roof, cooling occurs well into the daylight hours, despite the absorption of solar radiation by the roof. The two wet roof cases are clearly adequate, as would be anticipated in an area where evaporative cooling is widely used. However, the wetted roof would have several advantages over conventional evaporative cooling, alleviating the high humidity problems encountered with evaporative cooling, and allowing the house to be sealed against dust and pollen, avoiding common allergens.

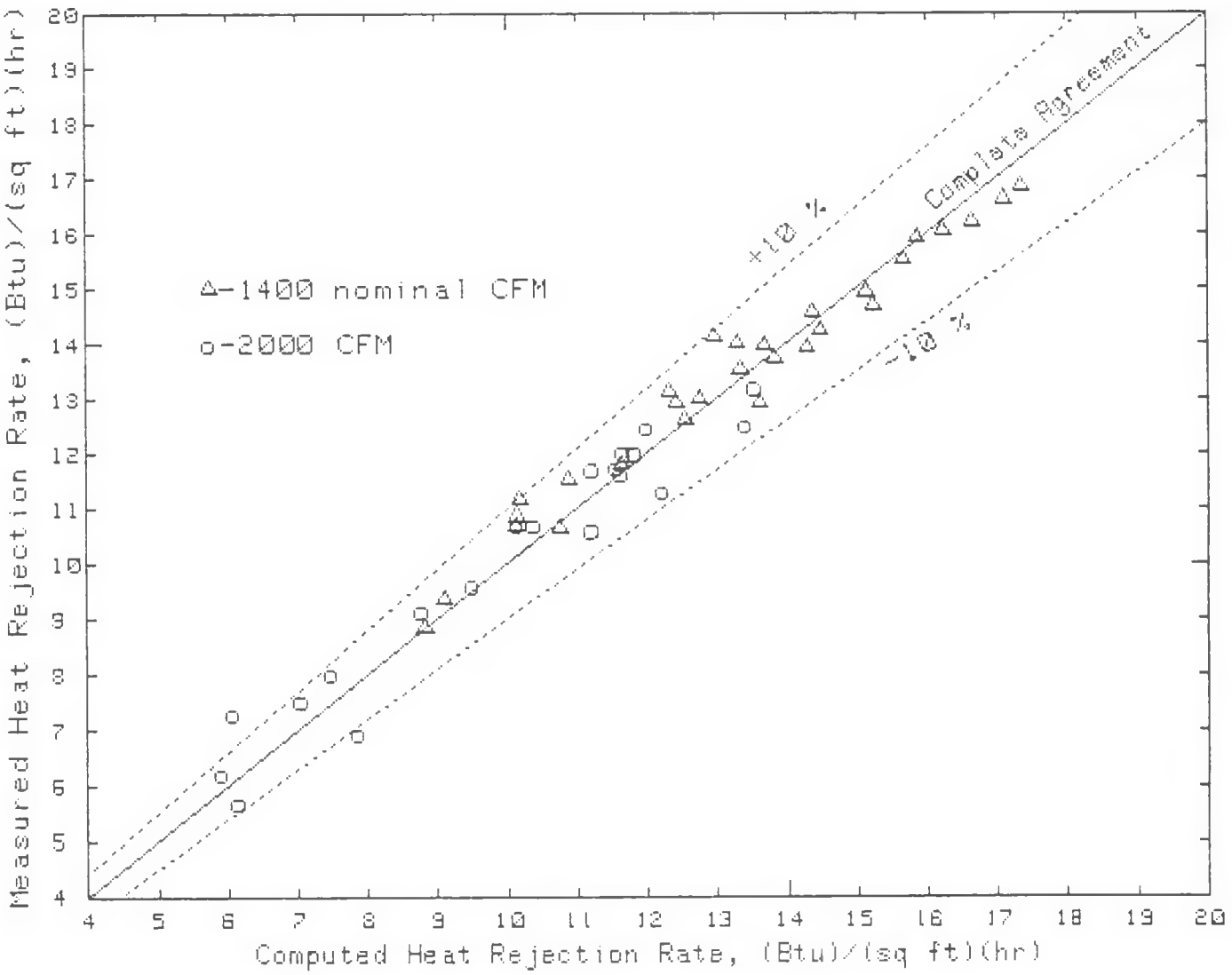

Figure 13. Comparison of computed and experimental values of roof heat rejection rates.

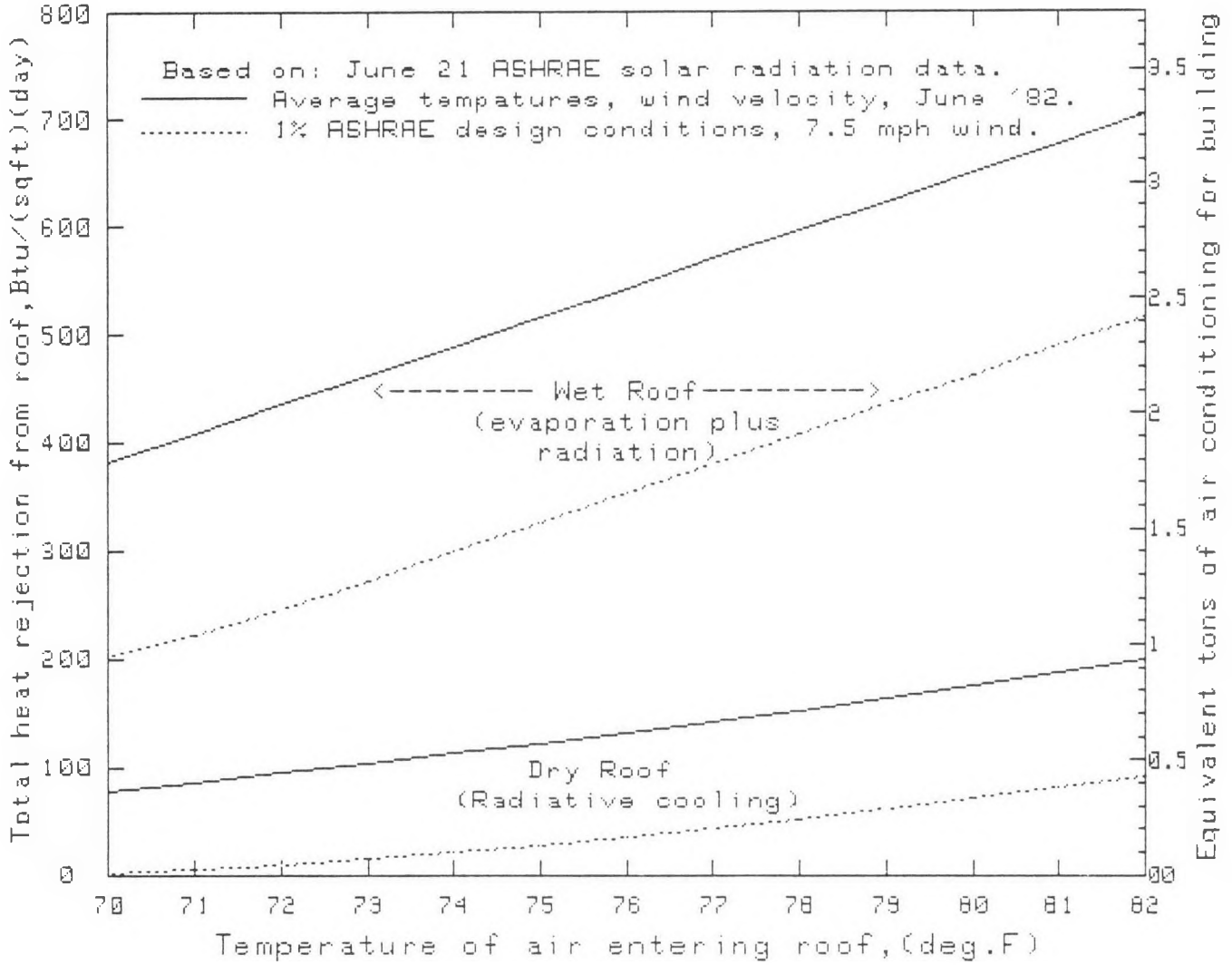

Figure 14. Typical roof performance.

Table III. Computed values of overall heat transfer coefficient (U_o) for experimental roof.

CFM ↓	Outside Combined Convective And Radiative Heat Transfer Coefficient 1.0	1.5	2.0	2.5	3.0	4.0	5.0	10.0	15.0	20.0
1000	.6628	.8508	.9914	1.1006	1.1879	1.3186	1.4120	1.6456	1.7424	1.7956
1200	.6989	.9112	1.0744	1.2038	1.3089	1.4694	1.5861	1.8866	2.0146	2.0857
1400	.7254	.9568	1.1384	1.2847	1.4052	1.5917	1.7296	2.0927	2.2509	2.3397
1600	.7461	.9930	1.1900	1.3508	1.4846	1.6944	1.8514	2.2734	2.4609	2.5672
1800	.7627	1.0227	1.2329	1.4064	1.5519	1.7826	1.9572	2.4346	2.6507	2.7742
2000	.7677	1.0317	1.2459	1.4233	1.5726	1.8099	1.9902	2.4858	2.7114	2.8406
2200	.7724	1.0402	1.2584	1.4397	1.5926	1.8364	2.0222	2.5359	2.7710	2.9060
2400	.7819	1.0576	1.2839	1.4730	1.6335	1.8910	2.0886	2.6410	2.8968	3.0445
2600	.7904	1.0732	1.3070	1.5035	1.6711	1.9415	2.1504	2.7403	3.0166	3.1770
2800	.7981	1.0874	1.3281	1.5315	1.7057	1.9884	2.2081	2.8345	3.1310	3.3040
3000	.8051	1.1004	1.3475	1.5574	1.7378	2.0322	2.2621	2.9241	3.2405	3.4260
4000	.8323	1.1518	1.4254	1.6624	1.8696	2.2147	2.4905	3.3167	3.7292	3.9766
5000	.8514	1.1887	1.4824	1.7404	1.9688	2.3552	2.6696	3.6419	4.1451	4.4528

Note: Air flow rate, cubic feet/min, is based on air at standard temperature ($70^{o}F$) and pressure (density = 0.075 lb/cu ft).

The outside combined convective and radiative heat transfer coefficient is ($h_{co} + \varepsilon h_r$) as explained in the text, Btu/sq ft hr ^{o}F.

The dimensions for U_o are also Btu/sq ft hr ^{o}F.

Table IV. Computed values of collector plate efficiency factor (F_R) for experimental roof.

CFM ↓	Outside Combined Convective And Radiative Heat Transfer Coefficient									
	1.0	1.5	2.0	2.5	3.0	4.0	5.0	10.0	15.0	20.0
1000	.4792	.3767	.3096	.2624	.2275	.1796	.1482	.0789	.0537	.0407
1200	.5244	.4203	.3498	.2992	.2611	.2079	.1726	.0930	.0636	.0483
1400	.5611	.4568	.3844	.3314	.2909	.2336	.1949	.1063	.0730	.0555
1600	.5914	.4880	.4146	.3599	.3177	.2570	.2155	.1189	.0819	.0625
1800	.6171	.5151	.4412	.3854	.3418	.2784	.2346	.1308	.0905	.0692
2000	.6332	.5325	.4588	.4025	.3583	.2934	.2482	.1396	.0970	.0743
2200	.6473	.5480	.4745	.4179	.3732	.3071	.2606	.1479	.1031	.0791
2400	.6634	.5658	.4926	.4358	.3904	.3229	.2750	.1574	.1101	.0846
2600	.6778	.5819	.5091	.4522	.4065	.3377	.2886	.1666	.1169	.0900
2800	.6909	.5966	.5244	.4674	.4214	.3517	.3015	.1754	.1235	.0952
3000	.7026	.6101	.5385	.4816	.4353	.3648	.3138	.1839	.1299	.1003
4000	.7485	.6637	.5957	.5401	.4938	.4211	.3669	.2224	.1593	.1240
5000	.7804	.7022	.6380	.5842	.5387	.4657	.4099	.2555	.1853	.1453

Note: Active area of roof, under which air is actually flowing, is 83% of total roof area.

To convert F_R from active area to total roof area basis, multiply above by 0.83.

Air flow rate, cubic feet/min, is based on air at standard temperature ($70^{o}F$) and pressure (density = 0.075 lb/cu ft).

Table V. Computed overall heat transfer coefficient (U_o), based on air flow rate per unit area.

CFM/(SQ FT)	Outside Combined Convective And Radiative Heat Transfer Coefficient									
L	1.0	1.5	2.0	2.5	3.0	4.0	5.0	10.0	15.0	20.0
.8	.6380	.8104	.9370	1.0340	1.1107	1.2242	1.3043	1.5014	1.5817	1.6255
1.0	.6859	.8892	1.0439	1.1657	1.2641	1.4131	1.5208	1.7951	1.9107	1.9746
1.2	.7187	.9451	1.1219	1.2638	1.3801	1.5597	1.6919	2.0378	2.1876	2.2715
1.4	.7431	.9877	1.1824	1.3410	1.4728	1.6790	1.8331	2.2458	2.4287	2.5322
1.6	.7621	1.0216	1.2313	1.4043	1.5494	1.7793	1.9532	2.4284	2.6434	2.7661
1.8	.7684	1.0331	1.2479	1.4259	1.5758	1.8141	1.9953	2.4937	2.7208	2.8509
2.0	.7744	1.0438	1.2637	1.4466	1.6010	1.8477	2.0359	2.5573	2.7966	2.9342
2.5	.7981	1.0874	1.3281	1.5315	1.7057	1.9884	2.2080	2.8344	3.1309	3.3038
3.0	.8161	1.1211	1.3787	1.5993	1.7901	2.1041	2.3515	3.0750	3.4266	3.6346
3.5	.8304	1.1483	1.4201	1.6551	1.8604	2.2018	2.4743	3.2880	3.6930	3.9355
4.0	.8422	1.1709	1.4547	1.7024	1.9203	2.2862	2.5813	3.4796	3.9363	4.2128
4.5	.8520	1.1900	1.4843	1.7431	1.9723	2.3602	2.6759	3.6537	4.1605	4.4705
5.0	.8604	1.2064	1.5100	1.7786	2.0179	2.4258	2.7606	3.8133	4.3686	4.7117

Note: The air flow rate per unit area (cu ft/min/sq ft) is based on the active area of the roof. The air is at standard temperature ($70^{o}F$) and pressure (density = 0.075 lb/cu ft).

The outside combined convective and radiative heat transfer coefficient is ($h_{co} + \epsilon h_r$) as explained in the text, Btu/sq ft hr ^{o}F.

Table VI. Computed values of collector plate efficiency factors (F_R), based on air flow rate per unit area.

CFM/(SQ FT) ↓	Outside Combined Convective And Radiative Heat Transfer Coefficient									
	1.0	1.5	2.0	2.5	3.0	4.0	5.0	10.0	15.0	20.0
.8	.4510	.3504	.2858	.2410	.2082	.1635	.1345	.0712	.0483	.0366
1.0	.5075	.4038	.3345	.2851	.2482	.1969	.1631	.0875	.0597	.0453
1.2	.5515	.4472	.3752	.3227	.2829	.2266	.1888	.1026	.0704	.0535
1.4	.5869	.4833	.4100	.3555	.3136	.2534	.2123	.1169	.0805	.0614
1.6	.6161	.5140	.4402	.3844	.3409	.2776	.2339	.1303	.0902	.0689
1.8	.6346	.5341	.4603	.4040	.3598	.2947	.2494	.1404	.0976	.0747
2.0	.6507	.5517	.4782	.4216	.3768	.3103	.2636	.1498	.1045	.0802
2.5	.6908	.5966	.5244	.4674	.4214	.3517	.3015	.1754	.1235	.0952
3.0	.7214	.6317	.5613	.5048	.4583	.3868	.3343	.1985	.1409	.1092
3.5	.7455	.6601	.5918	.5360	.4897	.4171	.3630	.2195	.1571	.1222
4.0	.7651	.6836	.6175	.5627	.5167	.4437	.3885	.2389	.1721	.1345
4.5	.7814	.7036	.6394	.5858	.5403	.4673	.4114	.2567	.1863	.1461
5.0	.7953	.7207	.6585	.6060	.5611	.4884	.4321	.2734	.1996	.1571

Note: The air flow rate per unit area (cu ft/min/sq ft) is based on the active area of the roof. The air is at standard temperature ($70^{o}F$) and pressure (density = 0.075 lb/cu ft).

The outside combined convective and radiative heat transfer coefficient is ($h_{co} + \epsilon h_r$) as explained in the text, Btu/sq ft hr ^{o}F.

Notes and References

1. R. W. Bliss, Jr. "The Performance of an Experimental System using Solar Energy for Heating and Night Radiation for Cooling a Building." United Nations Conference on New Sources of Energy, Rome, E/Conf. 35/S/30, 1961.

2. R. W. Bliss, Jr. "The Derivations of Several Plate-Efficiency Factors Useful in the Design of Flat-Plate Solar Heat Collectors." J. Solar Energy 3: No. 4, Dec. 1959, pp. 55-64.

3. American Society of Heating, Refrigerating, and Air-conditioning Engineers. ASHRAE Handbook and Product Directory, 1977 Fundamentals. ASHRAE, 345 E. 47th Street, New York, New York 10017, p. 25.4, 3.9., 13.15.

4. M. W. Kays and A. L. London. Compact Heat Exchangers. 2nd ed. McGraw-Hill Book Co., 1964, pp. 17, 18, 123, 14.

5. American Society of Heating, Refrigerating, and Air-conditioning Engineers. ASHRAE Handbook and Product Directory, 1979 Equipment. ASHRAE, 345 E. 47th Street, New York, N.Y. 10017, p. 4.4.

6. F. W. Hutchinson. Heating and Humidifying Load Analysis. Ronald Press, New York, N.Y., 1962, p. 109.

7. E.M. Sparrow, J. S. Nelson, and W. Q. Tao. "Effect of Leeward Orientation, Adiabatic Framing Surfaces, and Eaves on Solar-Collector Related Heat Transfer Coefficients." Solar Energy, Vol. 29, No. 1, 1982, pp. 33-41.

8. C. N. Hodges, et al. Solar Distillation Utilizing Multiple-effect Humidification. NTIS No. PB206068, Springfield, VA., 1966, pp. 60-90.

9. Eppley Precision Infrared Radiometer Model PIR, S/N 20480F3, the Eppley Laboratory, Inc., Newport, R.I. 02840.

10. Gill Propeller Vane Anemometer, Model No. 35003, R. M. Young Co., 28002 Aero-Park Dr., Traverse City, Michigan 49684.

11. P. Berdahl and R. Fromberg. "The Thermal Radiance of Clear Skies." Solar Energy, Vol. 29, No. 4, 1982, pp. 299-314.

12. W. D. Sellers. Physical Climatology, University of Chicago Press, Chicago, 1965.

13. Model F0P 15-9 CW, 1/2 hp, 1725/1140 RPM, Lau Industries, Div. of Philips Ind., 2027 Home Avenue, Dayton, Ohio 45407.

14. R. H. Perry and C. H. Chilton, ed., Chemical Engineers Handbook. 5th Ed. McGraw-Hill Book Co., New York, N. Y., 1973, p. 10-14.

15. W. H. McAdams. Heat Transmission, 3rd ed., McGraw-Hill Book Co., New York, N.Y., 1954, p. 62.

16. Local Climatological Data, Monthly Summary. June 1982, Tucson, Arizona. NOAA. National Climatic Center, Ashville, N.C.

Appendix I Experimental Data

September 18 and 19, 1982

October 9-12, 1982

Code	Instrument and Location
9WS001	Wind speed, mph, east side of facility
9WS002	Wind speed, mph, west side of facility
9AZ001	Wind direction, degrees, east
9AZ002	Wind direction, degrees, west
0PG001	Pyrgeometer, atmospheric radiation, Btu/sq ft hr
0PM004	Pyranometer, total horizontal solar radiation, Btu/sq ft hr
0PM005	Pyranometer, diffuse horizontal solar radiation, Btu/sq ft hr
9DT006	Thermocouple, ambient air temperature, ^{o}F
9WT006	Thermocouple, ambient air wet bulb temperature, ^{o}F
1ST104	Thermocouple, outlet air from roof, north end, east side, ^{o}F
1ST105	Thermocouple, outlet air from roof, north end, center, ^{o}F
1ST106	Thermocouple, outlet air from roof, north end, west side, ^{o}F
1ST107	Thermocouple, inlet air to roof, south end, east side, ^{o}F
1ST108	Thermocouple, inlet air to roof, south end, center, ^{o}F
1ST109	Thermocouple, inlet air to roof, south end, west, ^{o}F
1NT003	Thermocouple, air temperature in roof channel (2' from east side of roof), 2' from north outlet, ^{o}F

1NT004	Thermocouple, air temperature in same channel as INT003, 2' from south inlet, ^{o}F
1NT005	Thermocouple, air temperature in same channel as INT003, center, ^{o}F
1ST040	Thermocouple, roof surface, near INT003, ^{o}F
1ST041	Thermocouple, roof surface, near INT005, ^{o}F
1ST042	Thermocouple, roof surface, near INT004, ^{o}F
1CT011	Thermocouple, dry bulb air, 6" above floor, south living room, ^{o}F
1CT012	Thermocouple, dry bulb air, 2' above floor, south living room, ^{o}F
1CT013	Thermocouple, wet bulb air, 2' above floor, south living room, ^{o}F

INSTRUMENT DATA

Date	Time	9WS001	9AZ001	9WS002	9AZ002	0PG001
09/18	00:00	.58MPH	248.09deg	2.12MPH	288.62deg	121.07BTUH
09/18	01:00	1.11MPH	222.77deg	1.67MPH	206.12deg	117.42BTUH
09/18	02:00	1.12MPH	224.37deg	2.24MPH	87.55deg	107.73BTUH
09/18	03:00	.88MPH	218.75deg	1.05MPH	263.55deg	109.61BTUH
09/18	04:00	1.02MPH	321.91deg	1.22MPH	322.91deg	110.84BTUH
09/18	05:00	1.45MPH	45.81deg	1.77MPH	64.73deg	104.05BTUH
09/18	06:00	.37MPH	134.36deg	1.17MPH	12.72deg	103.00BTUH
09/18	07:00	1.33MPH	163.43deg	.91MPH	154.05deg	103.84BTUH
09/18	08:00	2.08MPH	179.99deg	2.90MPH	161.63deg	107.69BTUH
09/18	09:00	.76MPH	180.33deg	1.50MPH	166.27deg	112.78BTUH
09/18	10:00	1.38MPH	160.92deg	2.10MPH	147.50deg	118.15BTUH
09/18	11:00	1.27MPH	218.18deg	2.21MPH	200.04deg	123.17BTUH
09/18	12:00	1.33MPH	247.37deg	3.33MPH	279.56deg	126.07BTUH
09/18	13:00	3.57MPH	325.91deg	3.78MPH	308.51deg	129.33BTUH
09/18	14:00	3.62MPH	228.55deg	5.52MPH	326.21deg	129.00BTUH
09/18	15:00	4.50MPH	329.42deg	6.34MPH	316.07deg	128.06BTUH
09/18	16:00	6.59MPH	328.84deg	7.78MPH	315.68deg	126.14BTUH
09/18	17:00	5.26MPH	328.95deg	6.21MPH	306.10deg	123.88BTUH
09/18	18:00	6.74MPH	331.41deg	6.08MPH	301.37deg	120.24BTUH
09/18	19:00	3.84MPH	304.63deg	3.99MPH	297.15deg	117.62BTUH
09/18	20:00	3.19MPH	321.79deg	4.38MPH	295.46deg	116.43BTUH
09/18	21:00	3.64MPH	237.22deg	5.08MPH	294.04deg	115.77BTUH
09/18	22:00	1.23MPH	211.65deg	3.57MPH	262.16deg	114.69BTUH
09/18	23:00	1.52MPH	169.25deg	3.06MPH	143.11deg	111.70BTUH
09/19	00:00	1.89MPH	138.09deg	3.28MPH	116.00deg	111.09BTUH
09/19	01:00	.98MPH	153.40deg	3.00MPH	134.97deg	109.85BTUH
09/19	02:00	1.73MPH	104.39deg	2.23MPH	89.58deg	108.84BTUH
09/19	03:00	1.48MPH	115.79deg	2.69MPH	325.68deg	108.27BTUH
09/19	04:00	3.35MPH	195.86deg	4.07MPH	183.98deg	107.70BTUH
09/19	05:00	2.45MPH	235.07deg	4.54MPH	90.81deg	106.72BTUH
09/19	06:00	2.05MPH	179.53deg	3.69MPH	86.98deg	106.53BTUH
09/19	07:00	2.63MPH	132.98deg	3.80MPH	108.14deg	108.10BTUH
09/19	08:00	.51MPH	191.55deg	4.30MPH	154.36deg	114.84BTUH
09/19	09:00	4.42MPH	162.94deg	7.09MPH	96.88deg	117.65BTUH
09/19	10:00	6.74MPH	214.90deg	10.75MPH	90.83deg	121.15BTUH
09/19	11:00	3.82MPH	88.67deg	9.29MPH	83.22deg	125.54BTUH
09/19	12:00	3.80MPH	189.97deg	8.24MPH	258.52deg	128.81BTUH
09/19	13:00	3.15MPH	160.94deg	3.87MPH	187.66deg	130.48BTUH
09/19	14:00	4.54MPH	156.49deg	4.19MPH	192.69deg	127.66BTUH
09/19	15:00	4.83MPH	192.87deg	5.76MPH	184.36deg	127.91BTUH
09/19	16:00	2.91MPH	183.26deg	5.00MPH	223.48deg	124.64BTUH
09/19	17:00	2.67MPH	244.11deg	2.88MPH	240.21deg	122.46BTUH
09/19	18:00	1.72MPH	285.28deg	4.58MPH	271.07deg	119.49BTUH
09/19	19:00	2.85MPH	322.44deg	3.56MPH	316.95deg	117.54BTUH
09/19	20:00	2.45MPH	342.18deg	1.99MPH	329.43deg	117.18BTUH
09/19	21:00	.36MPH	317.23deg	3.48MPH	267.28deg	117.35BTUH
09/19	22:00	1.77MPH	248.94deg	2.87MPH	249.68deg	115.69BTUH
09/19	23:00	3.44MPH	203.79deg	3.31MPH	199.67deg	112.86BTUH

INSTRUMENT DATA

Date	Time	0PM004	0PM005	1VA001	9DT006	9WT006
09/18	00:00	0.00BTUH	0.00BTUH	1.82MPH	67.94F	62.06F
09/18	01:00	0.00BTUH	0.00BTUH	1.82MPH	67.90F	62.33F
09/18	02:00	0.00BTUH	0.00BTUH	1.83MPH	65.86F	62.46F
09/18	03:00	0.00BTUH	0.00BTUH	1.84MPH	65.37F	62.13F
09/18	04:00	0.00BTUH	0.00BTUH	1.84MPH	65.00F	62.11F
09/18	05:00	0.00BTUH	0.00BTUH	1.84MPH	63.32F	61.29F
09/18	06:00	0.00BTUH	0.00BTUH	1.84MPH	62.88F	60.68F
09/18	07:00	14.16BTUH	7.94BTUH	1.85MPH	63.06F	60.81F
09/18	08:00	60.59BTUH	20.34BTUH	1.87MPH	65.93F	61.92F
09/18	09:00	130.70BTUH	27.99BTUH	1.89MPH	70.37F	63.53F
09/18	10:00	188.61BTUH	32.68BTUH	1.90MPH	76.92F	65.46F
09/18	11:00	233.13BTUH	35.70BTUH	1.91MPH	80.57F	66.55F
09/18	12:00	260.69BTUH	37.29BTUH	1.92MPH	84.66F	67.83F
09/18	13:00	266.56BTUH	38.06BTUH	1.93MPH	87.00F	67.70F
09/18	14:00	249.55BTUH	37.46BTUH	1.93MPH	89.58F	67.73F
09/18	15:00	210.58BTUH	35.70BTUH	1.93MPH	91.06F	68.78F
09/18	16:00	161.36BTUH	32.38BTUH	1.92MPH	90.28F	68.59F
09/18	17:00	96.84BTUH	26.63BTUH	1.92MPH	89.85F	67.89F
09/18	18:00	34.32BTUH	15.26BTUH	1.90MPH	88.02F	66.86F
09/18	19:00	0.00BTUH	0.00BTUH	1.88MPH	84.92F	66.18F
09/18	20:00	0.00BTUH	0.00BTUH	1.86MPH	82.45F	65.98F
09/18	21:00	0.00BTUH	0.00BTUH	1.86MPH	80.95F	65.50F
09/18	22:00	0.00BTUH	0.00BTUH	1.87MPH	79.64F	64.98F
09/18	23:00	0.00BTUH	0.00BTUH	1.86MPH	75.32F	64.32F
09/19	00:00	0.00BTUH	0.00BTUH	1.86MPH	72.39F	63.42F
09/19	01:00	0.00BTUH	0.00BTUH	1.86MPH	72.14F	63.07F
09/19	02:00	0.00BTUH	0.00BTUH	1.85MPH	69.64F	62.40F
09/19	03:00	0.00BTUH	0.00BTUH	1.85MPH	68.25F	61.83F
09/19	04:00	0.00BTUH	0.00BTUH	1.85MPH	67.76F	61.35F
09/19	05:00	0.00BTUH	0.00BTUH	1.85MPH	66.28F	60.80F
09/19	06:00	0.00BTUH	0.00BTUH	1.85MPH	65.57F	60.35F
09/19	07:00	13.40BTUH	7.86BTUH	1.86MPH	67.57F	60.87F
09/19	08:00	95.50BTUH	23.49BTUH	1.90MPH	73.84F	63.87F
09/19	09:00	132.73BTUH	27.20BTUH	1.90MPH	78.92F	66.25F
09/19	10:00	192.73BTUH	31.64BTUH	1.90MPH	83.27F	67.19F
09/19	11:00	238.75BTUH	33.81BTUH	1.91MPH	86.20F	68.71F
09/19	12:00	265.07BTUH	35.04BTUH	1.93MPH	89.30F	69.74F
09/19	13:00	274.05BTUH	36.26BTUH	1.94MPH	93.09F	68.10F
09/19	14:00	256.63BTUH	37.03BTUH	1.95MPH	94.60F	66.90F
09/19	15:00	218.69BTUH	38.40BTUH	1.93MPH	95.32F	67.88F
09/19	16:00	144.63BTUH	32.00BTUH	1.94MPH	96.09F	67.74F
09/19	17:00	95.59BTUH	24.68BTUH	1.94MPH	95.41F	67.45F
09/19	18:00	33.01BTUH	14.13BTUH	1.93MPH	93.66F	66.98F
09/19	19:00	0.00BTUH	0.00BTUH	1.90MPH	88.78F	67.03F
09/19	20:00	0.00BTUH	0.00BTUH	1.89MPH	85.31F	66.82F
09/19	21:00	0.00BTUH	0.00BTUH	1.88MPH	84.14F	66.13F
09/19	22:00	0.00BTUH	0.00BTUH	1.88MPH	82.13F	65.19F
09/19	23:00	0.00BTUH	0.00BTUH	1.87MPH	79.07F	62.47F

INSTRUMENT DATA

Date	Time	1ST104	1ST105	1ST106	1ST107	1ST108
09/18	00:00	67.33F	68.01F	67.34F	72.75F	72.62F
09/18	01:00	67.36F	67.97F	67.28F	72.72F	72.60F
09/18	02:00	64.23F	64.92F	64.02F	71.43F	71.29F
09/18	03:00	63.01F	63.92F	62.89F	70.56F	70.43F
09/18	04:00	63.74F	64.57F	63.66F	70.59F	70.46F
09/18	05:00	61.70F	62.46F	61.47F	69.64F	69.51F
09/18	06:00	60.31F	61.24F	60.12F	68.77F	68.63F
09/18	07:00	60.46F	61.38F	60.30F	68.42F	68.31F
09/18	08:00	64.50F	65.30F	64.38F	69.64F	69.51F
09/18	09:00	72.61F	72.75F	72.61F	73.02F	72.85F
09/18	10:00	81.67F	81.02F	81.57F	77.50F	77.35F
09/18	11:00	89.25F	88.14F	89.08F	82.02F	81.82F
09/18	12:00	94.22F	92.78F	93.70F	85.42F	85.07F
09/18	13:00	96.46F	95.01F	95.86F	87.65F	87.25F
09/18	14:00	97.36F	96.05F	96.91F	89.00F	88.51F
09/18	15:00	96.15F	95.04F	95.74F	89.40F	88.85F
09/18	16:00	92.34F	91.64F	92.14F	88.19F	87.68F
09/18	17:00	87.98F	87.61F	87.91F	86.25F	85.74F
09/18	18:00	82.81F	82.74F	82.86F	83.71F	83.24F
09/18	19:00	77.82F	78.13F	77.99F	81.03F	80.65F
09/18	20:00	75.07F	75.62F	75.40F	79.29F	79.01F
09/18	21:00	73.75F	74.35F	74.09F	78.26F	78.02F
09/18	22:00	71.98F	72.65F	72.21F	77.29F	77.05F
09/18	23:00	69.66F	70.30F	69.58F	75.98F	75.76F
09/19	00:00	67.95F	68.61F	67.72F	74.78F	74.60F
09/19	01:00	67.37F	68.05F	67.22F	74.25F	74.08F
09/19	02:00	66.01F	66.69F	65.76F	73.36F	73.24F
09/19	03:00	64.97F	65.72F	64.74F	72.66F	72.49F
09/19	04:00	64.67F	65.39F	64.51F	72.20F	72.05F
09/19	05:00	64.05F	64.77F	63.87F	71.73F	71.59F
09/19	06:00	63.19F	63.91F	62.96F	71.07F	70.97F
09/19	07:00	64.28F	64.95F	64.13F	71.16F	71.02F
09/19	08:00	72.24F	72.41F	72.19F	74.15F	73.97F
09/19	09:00	77.54F	77.34F	77.50F	76.58F	76.40F
09/19	10:00	84.93F	84.45F	85.09F	80.79F	80.58F
09/19	11:00	90.15F	89.67F	90.55F	84.24F	84.01F
09/19	12:00	95.07F	94.51F	95.68F	87.53F	87.23F
09/19	13:00	99.32F	98.19F	99.38F	90.22F	89.85F
09/19	14:00	100.28F	99.10F	100.20F	91.65F	91.24F
09/19	15:00	98.94F	97.92F	98.82F	91.90F	91.44F
09/19	16:00	95.58F	94.78F	95.47F	91.02F	90.54F
09/19	17:00	90.40F	89.94F	90.30F	88.77F	88.25F
09/19	18:00	84.75F	84.79F	84.90F	86.06F	85.58F
09/19	19:00	79.95F	80.27F	80.17F	83.32F	82.90F
09/19	20:00	76.36F	76.78F	76.32F	81.10F	80.77F
09/19	21:00	74.68F	75.39F	74.93F	79.88F	79.60F
09/19	22:00	73.47F	74.20F	73.71F	79.09F	78.83F
09/19	23:00	71.95F	72.66F	71.98F	78.09F	77.85F

INSTRUMENT- DATA

Date	Time	1ST109	1NT003	1NT004	1NT005	1ST040
09/18	00:00	72.79F	67.91F	71.69F	70.08F	65.09F
09/18	01:00	72.76F	67.89F	71.69F	70.03F	64.99F
09/18	02:00	71.43F	64.87F	70.03F	67.72F	61.21F
09/18	03:00	70.59F	63.88F	69.15F	66.90F	60.05F
09/18	04:00	70.62F	64.53F	69.28F	67.22F	60.90F
09/18	05:00	69.67F	62.43F	68.07F	65.58F	58.63F
09/18	06:00	68.78F	61.18F	67.19F	64.59F	56.90F
09/18	07:00	68.45F	61.46F	66.98F	64.60F	57.69F
09/18	08:00	69.70F	65.80F	68.76F	67.53F	63.59F
09/18	09:00	73.05F	73.59F	72.95F	73.31F	74.25F
09/18	10:00	77.49F	81.99F	78.17F	79.93F	84.69F
09/18	11:00	81.97F	89.03F	83.26F	85.93F	92.91F
09/18	12:00	85.17F	93.61F	86.98F	90.15F	97.39F
09/18	13:00	87.33F	95.76F	89.25F	92.40F	99.07F
09/18	14:00	88.57F	96.54F	90.52F	93.45F	99.29F
09/18	15:00	88.90F	95.29F	90.57F	92.89F	97.51F
09/18	16:00	87.63F	91.58F	88.85F	90.20F	92.94F
09/18	17:00	85.77F	87.34F	86.36F	86.84F	88.15F
09/18	18:00	83.34F	82.45F	83.29F	82.88F	82.44F
09/18	19:00	80.76F	77.96F	80.21F	79.12F	77.07F
09/18	20:00	79.14F	75.45F	78.36F	77.01F	74.08F
09/18	21:00	78.17F	74.21F	77.29F	75.86F	72.86F
09/18	22:00	77.16F	72.58F	76.18F	74.53F	70.37F
09/18	23:00	75.88F	70.27F	74.72F	72.78F	67.36F
09/19	00:00	74.74F	68.64F	73.49F	71.35F	65.62F
09/19	01:00	74.24F	68.05F	72.95F	70.82F	64.79F
09/19	02:00	73.38F	66.81F	71.95F	69.69F	63.49F
09/19	03:00	72.62F	65.80F	71.19F	68.82F	62.23F
09/19	04:00	72.20F	65.46F	70.73F	68.39F	62.24F
09/19	05:00	71.75F	64.85F	70.19F	67.82F	61.39F
09/19	06:00	71.13F	64.01F	69.52F	67.08F	60.50F
09/19	07:00	71.20F	65.21F	69.85F	67.79F	62.71F
09/19	08:00	74.10F	73.08F	73.79F	73.52F	73.08F
09/19	09:00	76.55F	78.12F	76.76F	77.46F	79.56F
09/19	10:00	80.68F	85.01F	81.61F	83.24F	87.03F
09/19	11:00	84.06F	89.94F	85.41F	87.59F	92.38F
09/19	12:00	87.33F	94.57F	89.04F	91.72F	97.36F
09/19	13:00	89.97F	98.61F	91.92F	95.06F	102.50F
09/19	14:00	91.33F	99.40F	93.20F	96.08F	103.02F
09/19	15:00	91.52F	97.95F	93.11F	95.38F	100.72F
09/19	16:00	90.54F	94.67F	91.73F	93.14F	96.41F
09/19	17:00	88.26F	89.70F	88.86F	89.25F	90.55F
09/19	18:00	85.63F	84.63F	85.63F	85.15F	84.43F
09/19	19:00	83.01F	80.08F	82.48F	81.32F	79.12F
09/19	20:00	80.87F	76.52F	80.01F	78.36F	75.12F
09/19	21:00	79.72F	75.29F	78.81F	77.20F	73.43F
09/19	22:00	78.97F	74.15F	77.95F	76.25F	71.83F
09/19	23:00	77.98F	72.71F	76.82F	75.01F	70.03F

INSTRUMENT DATA

Date	Time	1ST041	1ST042	1CT011	1CT012	1CT013
09/18	00:00	65.66F	67.42F	72.69F	72.50F	62.62F
09/18	01:00	65.79F	67.19F	72.46F	72.34F	62.59F
09/18	02:00	62.50F	63.95F	71.21F	70.74F	62.02F
09/18	03:00	61.70F	63.42F	70.21F	69.79F	61.48F
09/18	04:00	62.16F	63.77F	70.19F	69.93F	61.54F
09/18	05:00	59.92F	61.38F	69.32F	68.88F	61.02F
09/18	06:00	58.53F	60.33F	68.39F	67.89F	60.44F
09/18	07:00	59.47F	61.36F	68.13F	67.62F	60.20F
09/18	08:00	65.80F	66.75F	69.49F	69.24F	60.95F
09/18	09:00	75.23F	75.51F	72.70F	72.49F	62.71F
09/18	10:00	84.17F	84.14F	75.77F	76.38F	65.00F
09/18	11:00	91.75F	91.77F	77.58F	78.99F	66.74F
09/18	12:00	96.05F	96.39F	78.51F	80.73F	68.04F
09/18	13:00	97.67F	98.49F	79.56F	81.81F	69.07F
09/18	14:00	97.64F	98.57F	80.45F	83.06F	69.61F
09/18	15:00	96.58F	97.33F	81.17F	83.98F	70.01F
09/18	16:00	92.71F	93.23F	82.13F	84.38F	70.22F
09/18	17:00	88.42F	88.35F	82.29F	83.88F	69.74F
09/18	18:00	83.12F	82.91F	81.30F	82.09F	68.42F
09/18	19:00	78.37F	77.85F	80.09F	80.34F	67.11F
09/18	20:00	75.60F	75.45F	78.68F	78.66F	66.13F
09/18	21:00	74.36F	74.29F	77.76F	77.70F	65.57F
09/18	22:00	72.05F	72.24F	76.69F	76.70F	65.01F
09/18	23:00	69.21F	70.11F	75.38F	75.30F	64.33F
09/19	00:00	67.31F	68.37F	74.35F	73.92F	63.72F
09/19	01:00	66.63F	67.82F	73.81F	73.37F	63.36F
09/19	02:00	65.23F	66.32F	72.84F	72.61F	62.92F
09/19	03:00	63.99F	65.30F	68.60F	71.82F	62.51F
09/19	04:00	63.81F	65.09F	71.84F	71.44F	62.24F
09/19	05:00	62.78F	64.14F	71.20F	70.91F	61.90F
09/19	06:00	62.05F	63.40F	32.00F	70.27F	61.50F
09/19	07:00	64.37F	65.41F	70.81F	70.42F	61.47F
09/19	08:00	74.15F	74.59F	73.92F	73.70F	63.11F
09/19	09:00	80.03F	80.08F	75.85F	76.13F	64.42F
09/19	10:00	86.64F	86.71F	78.47F	79.46F	66.46F
09/19	11:00	91.37F	91.94F	79.91F	81.36F	67.92F
09/19	12:00	96.41F	96.54F	80.59F	82.52F	69.06F
09/19	13:00	100.69F	101.08F	81.76F	84.22F	70.11F
09/19	14:00	101.43F	101.62F	82.58F	85.42F	70.48F
09/19	15:00	99.50F	99.97F	83.46F	86.28F	70.79F
09/19	16:00	96.05F	96.18F	83.87F	86.84F	70.88F
09/19	17:00	91.14F	90.90F	84.47F	86.45F	70.45F
09/19	18:00	85.55F	85.33F	83.49F	84.47F	69.15F
09/19	19:00	80.63F	79.98F	82.09F	82.56F	67.94F
09/19	20:00	76.86F	76.27F	80.26F	80.41F	66.89F
09/19	21:00	75.20F	75.37F	79.00F	79.17F	66.17F
09/19	22:00	73.64F	74.13F	78.37F	78.43F	65.69F
09/19	23:00	71.74F	72.39F	77.54F	77.39F	64.90F

INSTRUMENT DATA

Date	Time	9WS001	9AZ001	9WS002	9AZ002	0PG001
10/09	00:00	1.61MPH	119.35deg	3.13MPH	103.74deg	83.01BTUH
10/09	01:00	1.72MPH	124.64deg	2.99MPH	94.40deg	81.90BTUH
10/09	02:00	1.39MPH	128.37deg	2.87MPH	95.97deg	81.13BTUH
10/09	03:00	.57MPH	177.46deg	1.11MPH	198.27deg	80.27BTUH
10/09	04:00	1.02MPH	175.26deg	1.64MPH	143.75deg	79.90BTUH
10/09	05:00	1.33MPH	80.97deg	3.01MPH	259.91deg	77.93BTUH
10/09	06:00	1.02MPH	175.83deg	2.08MPH	231.78deg	78.40BTUH
10/09	07:00	1.07MPH	187.52deg	1.05MPH	44.81deg	78.51BTUH
10/09	08:00	2.22MPH	129.31deg	1.41MPH	301.29deg	83.29BTUH
10/09	09:00	.97MPH	344.91deg	2.67MPH	329.69deg	88.10BTUH
10/09	10:00	3.47MPH	340.24deg	5.06MPH	306.62deg	93.88BTUH
10/09	11:00	4.74MPH	273.29deg	5.01MPH	324.33deg	97.57BTUH
10/09	12:00	3.96MPH	267.13deg	4.81MPH	346.69deg	99.52BTUH
10/09	13:00	4.65MPH	339.64deg	6.50MPH	335.46deg	101.31BTUH
10/09	14:00	3.83MPH	330.50deg	6.34MPH	328.89deg	100.49BTUH
10/09	15:00	6.63MPH	273.02deg	6.40MPH	307.52deg	98.47BTUH
10/09	16:00	4.11MPH	242.28deg	5.10MPH	305.19deg	96.34BTUH
10/09	17:00	3.68MPH	298.65deg	7.47MPH	289.86deg	93.27BTUH
10/09	18:00	1.28MPH	244.12deg	8.46MPH	280.99deg	89.72BTUH
10/09	19:00	2.14MPH	250.18deg	5.26MPH	257.08deg	86.97BTUH
10/09	20:00	3.01MPH	249.19deg	4.95MPH	257.50deg	86.19BTUH
10/09	21:00	2.49MPH	253.90deg	4.86MPH	258.15deg	85.18BTUH
10/09	22:00	1.53MPH	202.36deg	3.92MPH	298.44deg	83.80BTUH
10/09	23:00	1.36MPH	246.59deg	2.46MPH	64.28deg	81.92BTUH
10/10	00:00	1.98MPH	350.61deg	3.74MPH	90.05deg	80.09BTUH
10/10	01:00	1.25MPH	116.37deg	1.96MPH	113.52deg	79.98BTUH
10/10	02:00	.81MPH	133.22deg	1.64MPH	229.49deg	79.40BTUH
10/10	03:00	1.05MPH	212.16deg	1.98MPH	105.76deg	78.80BTUH
10/10	04:00	1.36MPH	171.28deg	1.77MPH	129.69deg	78.56BTUH
10/10	05:00	1.36MPH	105.82deg	1.74MPH	78.62deg	77.07BTUH
10/10	06:00	2.10MPH	111.72deg	2.31MPH	98.09deg	77.03BTUH
10/10	07:00	2.37MPH	117.11deg	2.85MPH	96.08deg	77.56BTUH
10/10	08:00	2.95MPH	156.46deg	5.48MPH	116.31deg	81.46BTUH
10/10	09:00	1.60MPH	198.77deg	2.68MPH	183.11deg	86.59BTUH
10/10	10:00	1.88MPH	244.35deg	3.33MPH	248.31deg	91.30BTUH
10/10	11:00	1.04MPH	255.73deg	2.52MPH	268.47deg	95.43BTUH
10/10	12:00	1.62MPH	269.93deg	1.48MPH	269.19deg	99.45BTUH
10/10	13:00	1.49MPH	331.13deg	3.99MPH	296.77deg	99.91BTUH
10/10	14:00	4.00MPH	273.20deg	5.59MPH	261.50deg	101.16BTUH
10/10	15:00	3.94MPH	279.91deg	7.17MPH	273.78deg	99.54BTUH
10/10	16:00	3.16MPH	356.01deg	6.73MPH	287.10deg	96.44BTUH
10/10	17:00	4.77MPH	277.48deg	6.73MPH	301.68deg	92.93BTUH
10/10	18:00	4.88MPH	333.08deg	6.22MPH	309.13deg	89.36BTUH
10/10	19:00	4.51MPH	320.25deg	5.11MPH	310.82deg	86.94BTUH
10/10	20:00	1.65MPH	269.62deg	2.56MPH	304.52deg	85.72BTUH
10/10	21:00	.75MPH	169.08deg	1.67MPH	116.66deg	82.64BTUH
10/10	22:00	1.47MPH	201.22deg	2.95MPH	304.18deg	81.77BTUH
10/10	23:00	2.83MPH	156.41deg	3.58MPH	139.99deg	80.92BTUH

INSTRUMENT DATA

Date	Time	0PM004	0PM005	1VA001	9DT006	9WT006
10/09	00:00	0.00BTUH	0.00BTUH	1.95MPH	52.70F	40.51F
10/09	01:00	0.00BTUH	0.00BTUH	1.95MPH	50.21F	39.02F
10/09	02:00	0.00BTUH	0.00BTUH	1.95MPH	47.55F	37.74F
10/09	03:00	0.00BTUH	0.00BTUH	1.95MPH	46.93F	37.46F
10/09	04:00	0.00BTUH	0.00BTUH	1.95MPH	46.11F	37.26F
10/09	05:00	0.00BTUH	0.00BTUH	1.94MPH	42.79F	*****F
10/09	06:00	0.00BTUH	0.00BTUH	1.94MPH	42.67F	*****F
10/09	07:00	7.46BTUH	4.83BTUH	1.95MPH	42.58F	*****F
10/09	08:00	59.56BTUH	15.52BTUH	1.98MPH	48.87F	38.81F
10/09	09:00	125.97BTUH	21.67BTUH	2.00MPH	56.54F	43.03F
10/09	10:00	185.41BTUH	25.55BTUH	2.01MPH	63.35F	46.08F
10/09	11:00	228.83BTUH	27.61BTUH	2.02MPH	66.73F	47.65F
10/09	12:00	254.72BTUH	28.83BTUH	2.02MPH	70.09F	48.88F
10/09	13:00	257.50BTUH	29.07BTUH	2.02MPH	72.14F	49.73F
10/09	14:00	238.68BTUH	27.85BTUH	2.01MPH	74.10F	50.44F
10/09	15:00	198.45BTUH	25.75BTUH	2.02MPH	74.64F	50.53F
10/09	16:00	142.33BTUH	22.33BTUH	2.01MPH	75.42F	50.66F
10/09	17:00	76.81BTUH	17.24BTUH	2.00MPH	74.60F	50.33F
10/09	18:00	15.82BTUH	7.77BTUH	1.99MPH	72.04F	48.98F
10/09	19:00	0.00BTUH	0.00BTUH	1.98MPH	68.12F	47.24F
10/09	20:00	0.00BTUH	0.00BTUH	1.98MPH	65.50F	45.94F
10/09	21:00	0.00BTUH	0.00BTUH	1.97MPH	62.15F	44.39F
10/09	22:00	0.00BTUH	0.00BTUH	1.97MPH	59.50F	43.09F
10/09	23:00	0.00BTUH	0.00BTUH	1.96MPH	53.73F	40.70F
10/10	00:00	0.00BTUH	0.00BTUH	1.95MPH	48.40F	37.51F
10/10	01:00	0.00BTUH	0.00BTUH	1.95MPH	47.71F	37.09F
10/10	02:00	0.00BTUH	0.00BTUH	1.95MPH	46.08F	*****F
10/10	03:00	0.00BTUH	0.00BTUH	1.95MPH	44.38F	*****F
10/10	04:00	0.00BTUH	0.00BTUH	1.95MPH	45.21F	*****F
10/10	05:00	0.00BTUH	0.00BTUH	1.95MPH	43.16F	*****F
10/10	06:00	0.00BTUH	0.00BTUH	1.95MPH	41.45F	*****F
10/10	07:00	7.01BTUH	4.67BTUH	1.95MPH	42.48F	*****F
10/10	08:00	57.38BTUH	16.65BTUH	1.98MPH	48.18F	37.27F
10/10	09:00	134.49BTUH	24.76BTUH	2.00MPH	54.57F	41.26F
10/10	10:00	181.97BTUH	28.29BTUH	2.01MPH	59.59F	43.89F
10/10	11:00	224.98BTUH	31.12BTUH	2.02MPH	63.99F	46.18F
10/10	12:00	251.22BTUH	31.96BTUH	2.03MPH	68.24F	47.92F
10/10	13:00	254.47BTUH	32.45BTUH	2.03MPH	71.61F	49.78F
10/10	14:00	234.72BTUH	32.43BTUH	2.02MPH	74.50F	50.66F
10/10	15:00	194.83BTUH	29.99BTUH	2.01MPH	75.06F	50.53F
10/10	16:00	138.88BTUH	26.30BTUH	2.01MPH	74.35F	50.24F
10/10	17:00	73.95BTUH	20.11BTUH	2.00MPH	71.86F	49.12F
10/10	18:00	14.31BTUH	8.42BTUH	1.99MPH	69.40F	48.02F
10/10	19:00	0.00BTUH	0.00BTUH	1.98MPH	65.66F	46.38F
10/10	20:00	0.00BTUH	0.00BTUH	1.98MPH	62.72F	45.04F
10/10	21:00	0.00BTUH	0.00BTUH	1.96MPH	55.80F	42.21F
10/10	22:00	0.00BTUH	0.00BTUH	1.97MPH	53.95F	40.48F
10/10	23:00	0.00BTUH	0.00BTUH	1.97MPH	53.25F	39.76F

INSTRUMENT DATA

Date	Time	1ST104	1ST105	1ST106	1ST107	1ST108
10/09	00:00	48.29F	49.37F	47.97F	62.33F	62.25F
10/09	01:00	46.46F	47.57F	45.98F	61.23F	61.19F
10/09	02:00	45.29F	46.39F	44.81F	60.30F	60.27F
10/09	03:00	43.48F	45.02F	43.19F	59.38F	59.28F
10/09	04:00	43.13F	44.53F	42.80F	58.73F	58.66F
10/09	05:00	41.49F	42.96F	41.24F	57.72F	57.66F
10/09	06:00	41.03F	42.49F	40.81F	57.03F	57.05F
10/09	07:00	40.37F	42.12F	40.25F	56.51F	56.39F
10/09	08:00	45.64F	46.92F	45.55F	57.50F	57.37F
10/09	09:00	55.30F	55.80F	55.30F	60.78F	60.47F
10/09	10:00	64.85F	64.63F	64.72F	64.89F	64.31F
10/09	11:00	72.13F	71.58F	72.08F	69.00F	68.27F
10/09	12:00	77.37F	76.49F	77.08F	72.21F	71.29F
10/09	13:00	79.62F	78.78F	79.44F	74.39F	73.31F
10/09	14:00	79.69F	78.94F	79.51F	75.45F	74.29F
10/09	15:00	77.81F	77.24F	77.71F	75.42F	74.26F
10/09	16:00	74.09F	73.71F	74.01F	74.26F	73.23F
10/09	17:00	68.89F	68.85F	69.03F	72.09F	71.12F
10/09	18:00	63.05F	63.56F	63.58F	69.35F	68.57F
10/09	19:00	57.61F	58.42F	58.03F	66.57F	66.16F
10/09	20:00	55.35F	56.24F	55.74F	65.03F	64.72F
10/09	21:00	52.92F	53.84F	53.21F	63.70F	63.42F
10/09	22:00	50.94F	51.94F	51.16F	62.62F	62.39F
10/09	23:00	46.93F	48.14F	46.69F	60.91F	60.66F
10/10	00:00	45.21F	46.16F	44.66F	59.59F	59.51F
10/10	01:00	43.61F	44.86F	43.19F	58.59F	58.54F
10/10	02:00	42.32F	43.69F	41.94F	57.67F	57.60F
10/10	03:00	41.25F	42.80F	41.02F	56.89F	56.86F
10/10	04:00	40.94F	42.51F	40.82F	56.27F	56.23F
10/10	05:00	40.31F	41.72F	40.02F	55.64F	55.63F
10/10	06:00	39.33F	40.78F	39.04F	54.87F	54.87F
10/10	07:00	39.73F	41.08F	39.56F	54.45F	54.48F
10/10	08:00	45.05F	45.84F	44.91F	55.61F	55.56F
10/10	09:00	54.98F	55.28F	55.02F	59.20F	58.97F
10/10	10:00	62.68F	62.44F	62.59F	62.59F	62.14F
10/10	11:00	70.62F	69.79F	70.28F	66.87F	66.19F
10/10	12:00	76.61F	75.61F	76.44F	70.45F	69.57F
10/10	13:00	79.58F	78.39F	79.17F	72.96F	71.93F
10/10	14:00	79.56F	78.48F	79.04F	74.01F	72.95F
10/10	15:00	77.21F	76.43F	76.89F	73.81F	72.87F
10/10	16:00	73.32F	72.86F	73.20F	72.65F	71.84F
10/10	17:00	67.72F	67.63F	67.81F	70.30F	69.55F
10/10	18:00	61.10F	61.42F	61.37F	67.39F	66.67F
10/10	19:00	56.17F	56.58F	56.24F	64.65F	64.23F
10/10	20:00	51.85F	52.74F	52.06F	62.63F	62.32F
10/10	21:00	47.04F	48.09F	46.73F	60.49F	60.19F
10/10	22:00	45.79F	46.96F	45.51F	59.17F	59.05F
10/10	23:00	46.39F	47.20F	46.09F	58.64F	58.53F

INSTRUMENT DATA

Date	Time	1ST109	1NT003	1NT004	1NT005	1ST040
10/09	00:00	62.58F	49.61F	59.22F	54.68F	44.29F
10/09	01:00	61.56F	47.85F	58.00F	53.20F	42.08F
10/09	02:00	60.68F	46.63F	57.01F	52.08F	40.68F
10/09	03:00	59.68F	45.06F	56.08F	50.98F	38.12F
10/09	04:00	59.08F	44.69F	55.44F	50.44F	38.33F
10/09	05:00	58.10F	43.04F	54.28F	49.01F	36.41F
10/09	06:00	57.47F	42.63F	53.67F	48.49F	36.16F
10/09	07:00	56.85F	42.21F	53.21F	48.18F	*****F
10/09	08:00	57.72F	47.83F	55.14F	51.77F	44.16F
10/09	09:00	60.71F	57.11F	59.71F	58.52F	55.90F
10/09	10:00	64.49F	66.03F	64.92F	65.48F	66.51F
10/09	11:00	68.36F	72.98F	69.72F	71.43F	73.97F
10/09	12:00	71.46F	77.75F	73.34F	75.59F	78.94F
10/09	13:00	73.42F	79.73F	75.45F	77.69F	80.47F
10/09	14:00	74.43F	79.58F	76.22F	78.00F	80.06F
10/09	15:00	74.30F	77.55F	75.60F	76.65F	77.77F
10/09	16:00	73.19F	73.70F	73.75F	73.73F	73.52F
10/09	17:00	71.15F	68.60F	70.80F	69.66F	67.85F
10/09	18:00	68.67F	63.37F	67.38F	65.32F	61.50F
10/09	19:00	66.30F	58.53F	64.29F	61.42F	55.50F
10/09	20:00	64.91F	56.51F	62.68F	59.62F	53.57F
10/09	21:00	63.67F	54.08F	61.06F	57.67F	50.53F
10/09	22:00	62.71F	52.13F	59.88F	56.11F	47.91F
10/09	23:00	60.96F	48.20F	57.87F	53.42F	42.36F
10/10	00:00	59.87F	46.46F	56.31F	51.60F	41.05F
10/10	01:00	58.90F	45.06F	55.30F	50.55F	39.08F
10/10	02:00	57.99F	43.84F	54.35F	49.49F	37.75F
10/10	03:00	57.24F	42.84F	53.56F	48.60F	*****F
10/10	04:00	56.58F	42.59F	53.07F	48.21F	36.58F
10/10	05:00	56.01F	41.89F	52.34F	47.48F	35.64F
10/10	06:00	55.27F	40.91F	51.48F	46.53F	*****F
10/10	07:00	54.85F	41.42F	51.21F	46.59F	*****F
10/10	08:00	55.91F	46.77F	53.32F	50.16F	44.03F
10/10	09:00	59.21F	56.38F	58.30F	57.41F	55.70F
10/10	10:00	62.34F	63.66F	62.59F	63.20F	64.36F
10/10	11:00	66.34F	71.12F	67.62F	69.39F	72.65F
10/10	12:00	69.76F	76.75F	71.67F	74.18F	79.07F
10/10	13:00	72.07F	79.34F	74.27F	76.83F	81.28F
10/10	14:00	73.09F	79.07F	75.05F	77.10F	80.56F
10/10	15:00	72.90F	76.69F	74.32F	75.54F	77.48F
10/10	16:00	71.78F	72.87F	72.41F	72.65F	72.98F
10/10	17:00	69.58F	67.36F	69.21F	68.25F	66.69F
10/10	18:00	66.75F	61.26F	65.39F	63.27F	59.63F
10/10	19:00	64.36F	56.55F	62.25F	59.32F	54.44F
10/10	20:00	62.48F	52.63F	59.95F	56.39F	48.99F
10/10	21:00	60.41F	48.12F	57.56F	53.22F	42.26F
10/10	22:00	59.32F	47.10F	56.30F	52.07F	42.36F
10/10	23:00	58.83F	47.58F	55.92F	52.02F	43.69F

INSTRUMENT DATA

Date	Time	1ST041	1ST042	1CT011	1CT012	1CT013
10/09	00:00	47.01F	49.31F	60.98F	61.19F	47.93F
10/09	01:00	44.82F	47.50F	59.70F	59.96F	47.20F
10/09	02:00	43.29F	46.08F	58.88F	59.25F	46.54F
10/09	03:00	41.15F	44.78F	57.78F	58.01F	45.83F
10/09	04:00	41.30F	44.42F	57.01F	57.26F	45.37F
10/09	05:00	39.13F	42.38F	55.86F	56.17F	44.72F
10/09	06:00	38.91F	42.09F	54.94F	55.50F	44.27F
10/09	07:00	38.81F	42.34F	54.59F	55.11F	43.82F
10/09	08:00	47.01F	49.06F	56.42F	56.61F	44.57F
10/09	09:00	58.18F	59.04F	59.97F	59.96F	46.37F
10/09	10:00	67.19F	67.99F	63.57F	63.93F	48.63F
10/09	11:00	73.86F	75.01F	66.10F	66.73F	50.40F
10/09	12:00	78.35F	79.59F	67.48F	68.33F	51.49F
10/09	13:00	79.67F	81.36F	68.67F	69.68F	52.48F
10/09	14:00	79.57F	80.96F	69.55F	70.69F	53.18F
10/09	15:00	77.73F	78.87F	70.07F	70.89F	53.48F
10/09	16:00	74.32F	74.82F	70.69F	71.33F	53.69F
10/09	17:00	69.18F	68.09F	69.53F	70.36F	53.08F
10/09	18:00	63.57F	63.42F	67.51F	68.03F	51.66F
10/09	19:00	57.87F	58.28F	65.05F	65.61F	50.23F
10/09	20:00	55.80F	56.71F	63.69F	64.31F	49.30F
10/09	21:00	52.85F	53.93F	62.58F	63.03F	48.44F
10/09	22:00	50.35F	51.77F	61.36F	61.68F	47.68F
10/09	23:00	45.58F	48.23F	59.17F	59.71F	46.62F
10/10	00:00	43.48F	45.85F	58.30F	58.56F	45.88F
10/10	01:00	42.08F	44.79F	57.04F	57.41F	45.15F
10/10	02:00	40.74F	43.69F	56.01F	56.42F	44.53F
10/10	03:00	39.59F	42.76F	55.04F	55.64F	43.91F
10/10	04:00	39.68F	42.66F	54.54F	55.19F	43.53F
10/10	05:00	38.71F	41.65F	53.99F	54.49F	43.09F
10/10	06:00	37.62F	40.64F	53.89F	53.89F	42.59F
10/10	07:00	38.88F	41.38F	53.38F	53.59F	42.29F
10/10	08:00	46.05F	47.63F	55.02F	55.13F	42.97F
10/10	09:00	56.96F	57.93F	58.59F	58.69F	45.02F
10/10	10:00	65.24F	65.84F	61.31F	61.84F	46.87F
10/10	11:00	72.66F	73.34F	63.92F	64.54F	48.74F
10/10	12:00	78.15F	78.86F	65.49F	66.31F	49.99F
10/10	13:00	80.83F	81.39F	66.78F	67.95F	51.21F
10/10	14:00	80.09F	80.85F	67.69F	68.77F	51.96F
10/10	15:00	77.50F	78.19F	68.18F	69.27F	52.21F
10/10	16:00	73.69F	74.09F	68.66F	69.47F	52.44F
10/10	17:00	67.73F	67.00F	67.98F	68.76F	51.83F
10/10	18:00	61.44F	61.02F	65.58F	66.09F	50.29F
10/10	19:00	56.53F	56.10F	63.19F	63.83F	48.81F
10/10	20:00	51.73F	52.13F	61.59F	61.73F	47.60F
10/10	21:00	45.12F	47.97F	59.33F	59.59F	46.31F
10/10	22:00	45.61F	47.92F	57.72F	57.97F	45.47F
10/10	23:00	46.33F	48.15F	57.95F	57.97F	45.08F

INSTRUMENT DATA

Date	Time	9WS001	9AZ001	9WS002	9AZ002	0PG001
10/11	00:00	1.77MPH	134.78deg	2.02MPH	115.62deg	79.86BTUH
10/11	01:00	1.83MPH	136.13deg	2.55MPH	112.20deg	78.91BTUH
10/11	02:00	3.10MPH	134.53deg	4.49MPH	106.66deg	78.68BTUH
10/11	03:00	1.92MPH	210.12deg	4.22MPH	88.60deg	76.56BTUH
10/11	04:00	2.74MPH	113.48deg	3.17MPH	90.48deg	77.17BTUH
10/11	05:00	2.52MPH	132.76deg	3.89MPH	95.30deg	76.83BTUH
10/11	06:00	4.40MPH	136.70deg	4.91MPH	99.97deg	77.86BTUH
10/11	07:00	4.58MPH	136.17deg	5.11MPH	111.03deg	78.24BTUH
10/11	08:00	3.52MPH	135.46deg	4.40MPH	109.64deg	82.22BTUH
10/11	09:00	4.81MPH	148.51deg	7.03MPH	128.78deg	87.37BTUH
10/11	10:00	2.87MPH	162.30deg	3.77MPH	136.39deg	93.81BTUH
10/11	11:00	1.50MPH	261.11deg	1.18MPH	198.25deg	98.51BTUH
10/11	12:00	2.30MPH	227.22deg	3.06MPH	315.75deg	100.17BTUH
10/11	13:00	2.67MPH	271.25deg	5.52MPH	250.22deg	100.42BTUH
10/11	14:00	1.53MPH	256.06deg	7.47MPH	296.11deg	99.80BTUH
10/11	15:00	5.28MPH	279.12deg	5.37MPH	262.08deg	99.55BTUH
10/11	16:00	3.34MPH	296.12deg	8.55MPH	279.65deg	97.20BTUH
10/11	17:00	5.01MPH	332.39deg	7.65MPH	295.70deg	94.72BTUH
10/11	18:00	7.21MPH	343.51deg	5.61MPH	318.20deg	90.90BTUH
10/11	19:00	5.40MPH	332.65deg	5.84MPH	304.43deg	88.98BTUH
10/11	20:00	.55MPH	225.99deg	3.57MPH	277.73deg	87.72BTUH
10/11	21:00	1.43MPH	276.84deg	2.17MPH	245.81deg	86.44BTUH
10/11	22:00	.50MPH	269.56deg	.82MPH	141.61deg	83.27BTUH
10/11	23:00	.99MPH	249.74deg	1.61MPH	124.16deg	83.34BTUH
10/12	00:00	2.12MPH	143.83deg	3.11MPH	112.81deg	82.87BTUH
10/12	01:00	2.25MPH	119.63deg	4.33MPH	103.39deg	82.35BTUH
10/12	02:00	1.90MPH	174.75deg	4.00MPH	164.02deg	81.36BTUH
10/12	03:00	1.54MPH	142.23deg	3.62MPH	91.12deg	79.69BTUH
10/12	04:00	*****MPH	*****deg	*****MPH	*****deg	*****BTUH
10/12	05:00	*****MPH	*****deg	*****MPH	*****deg	*****BTUH
10/12	06:00	*****MPH	*****deg	*****MPH	*****deg	*****BTUH
10/12	07:00	*****MPH	*****deg	*****MPH	*****deg	*****BTUH
10/12	08:00	*****MPH	*****deg	*****MPH	*****deg	*****BTUH
10/12	09:00	3.24MPH	171.07deg	3.77MPH	152.44deg	88.80BTUH
10/12	10:00	1.31MPH	175.90deg	2.17MPH	138.96deg	93.27BTUH
10/12	11:00	1.69MPH	181.29deg	1.73MPH	232.59deg	97.31BTUH
10/12	12:00	3.14MPH	303.92deg	4.02MPH	281.29deg	99.81BTUH
10/12	13:00	3.80MPH	291.83deg	3.78MPH	307.13deg	101.18BTUH
10/12	14:00	3.48MPH	243.10deg	3.43MPH	299.34deg	101.42BTUH
10/12	15:00	3.29MPH	277.10deg	3.71MPH	327.10deg	99.76BTUH
10/12	16:00	4.85MPH	315.17deg	6.14MPH	312.06deg	97.20BTUH
10/12	17:00	3.04MPH	331.55deg	4.23MPH	326.63deg	95.08BTUH
10/12	18:00	2.92MPH	317.55deg	4.67MPH	307.76deg	91.01BTUH
10/12	19:00	2.60MPH	320.30deg	2.91MPH	306.94deg	89.02BTUH
10/12	20:00	.60MPH	235.09deg	1.40MPH	232.54deg	87.74BTUH
10/12	21:00	1.29MPH	351.00deg	1.62MPH	202.51deg	86.46BTUH
10/12	22:00	.88MPH	180.16deg	1.29MPH	110.55deg	83.75BTUH
10/12	23:00	1.64MPH	299.73deg	1.64MPH	103.62deg	83.01BTUH

INSTRUMENT DATA

Date	Time	0PM004	0PM005	1VA001	9DT006	9WT006
10/11	00:00	0.00BTUH	0.00BTUH	1.96MPH	50.97F	38.62F
10/11	01:00	0.00BTUH	0.00BTUH	1.96MPH	47.23F	36.68F
10/11	02:00	0.00BTUH	0.00BTUH	1.96MPH	46.20F	*****F
10/11	03:00	0.00BTUH	0.00BTUH	1.95MPH	43.51F	*****F
10/11	04:00	0.00BTUH	0.00BTUH	1.95MPH	43.20F	*****F
10/11	05:00	0.00BTUH	0.00BTUH	1.96MPH	44.12F	*****F
10/11	06:00	0.00BTUH	0.00BTUH	1.96MPH	45.71F	*****F
10/11	07:00	6.69BTUH	4.91BTUH	1.97MPH	46.36F	*****F
10/11	08:00	55.05BTUH	18.17BTUH	1.98MPH	49.31F	37.69F
10/11	09:00	122.25BTUH	26.42BTUH	2.00MPH	55.58F	41.18F
10/11	10:00	180.35BTUH	31.40BTUH	2.02MPH	62.80F	45.30F
10/11	11:00	220.53BTUH	34.30BTUH	2.04MPH	67.83F	47.73F
10/11	12:00	246.24BTUH	35.90BTUH	2.04MPH	70.60F	49.19F
10/11	13:00	250.63BTUH	36.04BTUH	2.02MPH	73.04F	50.16F
10/11	14:00	231.81BTUH	34.74BTUH	2.02MPH	74.03F	50.48F
10/11	15:00	190.71BTUH	31.96BTUH	2.02MPH	74.68F	50.85F
10/11	16:00	135.43BTUH	27.28BTUH	2.01MPH	75.16F	51.25F
10/11	17:00	71.21BTUH	20.23BTUH	2.00MPH	73.54F	50.53F
10/11	18:00	12.91BTUH	7.91BTUH	1.99MPH	69.80F	48.67F
10/11	19:00	0.00BTUH	0.00BTUH	1.98MPH	66.94F	47.20F
10/11	20:00	0.00BTUH	0.00BTUH	1.98MPH	64.32F	46.19F
10/11	21:00	0.00BTUH	0.00BTUH	1.98MPH	62.20F	45.01F
10/11	22:00	0.00BTUH	0.00BTUH	1.97MPH	56.45F	42.46F
10/11	23:00	0.00BTUH	0.00BTUH	1.97MPH	52.64F	40.41F
10/12	00:00	0.00BTUH	0.00BTUH	1.97MPH	52.06F	40.00F
10/12	01:00	0.00BTUH	0.00BTUH	1.97MPH	50.32F	38.97F
10/12	02:00	0.00BTUH	0.00BTUH	1.97MPH	50.15F	38.90F
10/12	03:00	0.00BTUH	0.00BTUH	1.96MPH	46.39F	36.82F
10/12	04:00	*****BTUH	*****BTUH	*****MPH	*****F	*****F
10/12	05:00	*****BTUH	*****BTUH	*****MPH	*****F	*****F
10/12	06:00	*****BTUH	*****BTUH	*****MPH	*****F	*****F
10/12	07:00	*****BTUH	*****BTUH	*****MPH	*****F	*****F
10/12	08:00	*****BTUH	*****BTUH	*****MPH	*****F	*****F
10/12	09:00	135.15BTUH	26.92BTUH	2.01MPH	57.26F	42.69F
10/12	10:00	177.37BTUH	30.55BTUH	2.02MPH	61.80F	45.29F
10/12	11:00	219.79BTUH	33.07BTUH	2.03MPH	67.45F	48.06F
10/12	12:00	243.72BTUH	34.49BTUH	2.03MPH	70.14F	49.41F
10/12	13:00	247.88BTUH	34.54BTUH	2.03MPH	72.28F	49.55F
10/12	14:00	228.12BTUH	33.73BTUH	2.03MPH	73.91F	50.15F
10/12	15:00	186.85BTUH	31.88BTUH	2.03MPH	73.81F	50.40F
10/12	16:00	130.20BTUH	28.07BTUH	2.01MPH	74.04F	50.53F
10/12	17:00	67.49BTUH	20.49BTUH	2.01MPH	73.28F	50.21F
10/12	18:00	11.72BTUH	7.80BTUH	2.00MPH	71.07F	48.86F
10/12	19:00	0.00BTUH	0.00BTUH	1.99MPH	66.99F	46.99F
10/12	20:00	0.00BTUH	0.00BTUH	1.98MPH	64.01F	45.69F
10/12	21:00	0.00BTUH	0.00BTUH	1.98MPH	60.13F	44.08F
10/12	22:00	0.00BTUH	0.00BTUH	1.97MPH	53.60F	40.81F
10/12	23:00	0.00BTUH	0.00BTUH	1.96MPH	49.94F	38.66F

INSTRUMENT DATA

Date	Time	1ST104	1ST105	1ST106	1ST107	1ST108
10/11	00:00	44.37F	45.44F	44.09F	57.84F	57.73F
10/11	01:00	43.01F	44.16F	42.67F	56.83F	56.73F
10/11	02:00	42.03F	43.11F	41.70F	56.01F	56.02F
10/11	03:00	41.16F	42.17F	40.66F	55.40F	55.37F
10/11	04:00	40.16F	41.25F	39.74F	54.55F	54.59F
10/11	05:00	40.37F	41.36F	39.98F	54.17F	54.18F
10/11	06:00	41.26F	42.10F	40.94F	54.04F	54.08F
10/11	07:00	42.23F	42.84F	41.84F	54.12F	54.11F
10/11	08:00	45.64F	46.20F	45.45F	54.96F	54.89F
10/11	09:00	54.15F	54.30F	54.17F	58.06F	57.91F
10/11	10:00	63.47F	63.24F	63.57F	62.28F	61.97F
10/11	11:00	72.40F	71.55F	72.32F	66.98F	66.27F
10/11	12:00	77.63F	76.54F	77.51F	70.45F	69.46F
10/11	13:00	79.80F	78.59F	79.40F	72.55F	71.49F
10/11	14:00	78.87F	77.79F	78.27F	73.25F	72.18F
10/11	15:00	77.14F	76.30F	76.79F	73.27F	72.23F
10/11	16:00	73.49F	72.98F	73.32F	72.31F	71.33F
10/11	17:00	68.39F	68.29F	68.56F	70.16F	69.35F
10/11	18:00	62.61F	62.58F	62.63F	67.29F	66.58F
10/11	19:00	57.81F	58.15F	58.04F	64.68F	64.29F
10/11	20:00	53.52F	54.41F	53.99F	62.80F	62.53F
10/11	21:00	49.57F	50.85F	50.02F	61.00F	60.72F
10/11	22:00	46.99F	48.11F	46.88F	59.56F	59.31F
10/11	23:00	44.72F	45.94F	44.46F	58.07F	57.88F
10/12	00:00	45.34F	46.39F	45.18F	57.66F	57.54F
10/12	01:00	44.88F	45.69F	44.45F	57.01F	56.98F
10/12	02:00	44.73F	45.61F	44.59F	56.70F	56.64F
10/12	03:00	42.95F	43.81F	42.54F	55.86F	55.86F
10/12	04:00	*****F	*****F	*****F	*****F	*****F
10/12	05:00	*****F	*****F	*****F	*****F	*****F
10/12	06:00	*****F	*****F	*****F	*****F	*****F
10/12	07:00	*****F	*****F	*****F	*****F	*****F
10/12	08:00	*****F	*****F	*****F	*****F	*****F
10/12	09:00	56.03F	56.09F	56.08F	58.58F	58.34F
10/12	10:00	63.01F	62.69F	63.01F	61.83F	61.43F
10/12	11:00	71.69F	70.88F	71.61F	66.51F	65.75F
10/12	12:00	77.13F	76.02F	76.91F	69.99F	68.99F
10/12	13:00	79.45F	78.36F	79.23F	72.33F	71.12F
10/12	14:00	79.56F	78.48F	79.18F	73.44F	72.13F
10/12	15:00	76.84F	76.08F	76.68F	73.38F	72.05F
10/12	16:00	72.64F	72.13F	72.51F	72.05F	70.90F
10/12	17:00	66.97F	66.84F	67.00F	69.70F	68.60F
10/12	18:00	60.74F	61.03F	61.03F	66.72F	65.77F
10/12	19:00	54.94F	55.57F	55.08F	63.66F	63.13F
10/12	20:00	50.21F	51.38F	50.51F	61.42F	61.03F
10/12	21:00	48.51F	49.75F	48.69F	60.14F	59.81F
10/12	22:00	45.45F	46.62F	45.31F	58.55F	58.30F
10/12	23:00	44.37F	45.38F	43.91F	57.41F	57.28F

INSTRUMENT DATA

Date	Time	1ST109	1NT003	1NT004	1NT005	1ST040
10/11	00:00	58.03F	45.64F	54.92F	50.62F	40.58F
10/11	01:00	57.06F	44.29F	53.81F	49.39F	39.08F
10/11	02:00	56.38F	43.50F	52.89F	48.42F	38.65F
10/11	03:00	55.72F	42.42F	52.11F	47.49F	36.96F
10/11	04:00	54.95F	41.53F	51.30F	46.66F	*****F
10/11	05:00	54.56F	41.72F	51.07F	46.61F	37.01F
10/11	06:00	54.45F	42.68F	51.14F	47.04F	38.89F
10/11	07:00	54.49F	43.53F	51.37F	47.57F	39.86F
10/11	08:00	55.22F	47.14F	52.91F	50.10F	44.91F
10/11	09:00	58.13F	55.33F	57.16F	56.28F	54.87F
10/11	10:00	62.13F	64.40F	62.52F	63.44F	65.78F
10/11	11:00	66.45F	72.98F	68.05F	70.48F	75.58F
10/11	12:00	69.64F	77.72F	71.86F	74.74F	80.01F
10/11	13:00	71.66F	79.38F	73.98F	76.69F	81.48F
10/11	14:00	72.31F	78.34F	74.28F	76.38F	79.60F
10/11	15:00	72.32F	76.58F	73.83F	75.23F	77.51F
10/11	16:00	71.35F	73.03F	72.15F	72.59F	73.34F
10/11	17:00	69.34F	68.03F	69.23F	68.62F	67.75F
10/11	18:00	66.62F	62.43F	65.54F	63.90F	61.69F
10/11	19:00	64.41F	58.10F	62.69F	60.30F	56.55F
10/11	20:00	62.65F	54.33F	60.53F	57.50F	50.65F
10/11	21:00	60.94F	51.01F	58.54F	54.98F	46.52F
10/11	22:00	59.54F	48.28F	56.88F	52.94F	42.73F
10/11	23:00	58.16F	46.16F	55.31F	51.14F	40.65F
10/12	00:00	57.82F	46.66F	55.01F	51.14F	42.11F
10/12	01:00	57.29F	46.15F	54.30F	50.43F	42.21F
10/12	02:00	56.93F	45.87F	54.07F	50.25F	41.70F
10/12	03:00	56.17F	44.15F	52.95F	48.80F	39.33F
10/12	04:00	*****F	*****F	*****F	*****F	*****F
10/12	05:00	*****F	*****F	*****F	*****F	*****F
10/12	06:00	*****F	*****F	*****F	*****F	*****F
10/12	07:00	*****F	*****F	*****F	*****F	*****F
10/12	08:00	*****F	*****F	*****F	*****F	*****F
10/12	09:00	58.49F	57.21F	57.98F	57.66F	57.13F
10/12	10:00	61.59F	64.07F	62.10F	63.10F	65.36F
10/12	11:00	65.98F	72.41F	67.66F	69.90F	74.83F
10/12	12:00	69.23F	77.25F	71.46F	74.32F	79.53F
10/12	13:00	71.27F	79.39F	73.78F	76.64F	81.12F
10/12	14:00	72.35F	79.22F	74.55F	76.90F	80.85F
10/12	15:00	72.12F	76.44F	73.77F	75.14F	77.00F
10/12	16:00	70.86F	72.22F	71.66F	71.96F	72.35F
10/12	17:00	68.62F	66.62F	68.46F	67.49F	65.98F
10/12	18:00	65.83F	60.94F	64.74F	62.79F	59.50F
10/12	19:00	63.22F	55.46F	61.36F	58.39F	52.93F
10/12	20:00	61.14F	51.25F	58.87F	55.31F	46.74F
10/12	21:00	59.98F	49.84F	57.58F	54.05F	44.81F
10/12	22:00	58.55F	46.75F	55.74F	51.65F	41.24F
10/12	23:00	57.53F	45.68F	54.52F	50.47F	40.73F

INSTRUMENT DATA

Date	Time	1ST041	1ST042	1CT011	1CT012	1CT013
10/11	00:00	43.69F	45.94F	56.64F	57.00F	44.46F
10/11	01:00	41.81F	44.32F	55.55F	56.18F	43.83F
10/11	02:00	41.45F	43.44F	54.82F	55.08F	43.24F
10/11	03:00	39.25F	41.72F	54.05F	54.37F	42.77F
10/11	04:00	38.95F	41.25F	52.99F	53.55F	42.22F
10/11	05:00	39.42F	41.45F	52.96F	53.42F	41.99F
10/11	06:00	41.22F	42.78F	53.38F	53.42F	41.93F
10/11	07:00	42.04F	43.50F	53.18F	53.55F	41.88F
10/11	08:00	46.78F	48.02F	54.18F	54.51F	42.32F
10/11	09:00	55.62F	56.54F	57.36F	57.60F	44.07F
10/11	10:00	65.93F	66.39F	60.60F	61.24F	46.13F
10/11	11:00	75.40F	75.45F	62.93F	63.77F	47.93F
10/11	12:00	79.15F	79.39F	64.44F	65.61F	49.35F
10/11	13:00	80.75F	81.17F	65.85F	67.04F	50.54F
10/11	14:00	79.17F	79.97F	66.72F	68.01F	51.09F
10/11	15:00	77.44F	78.01F	67.17F	68.15F	51.41F
10/11	16:00	73.95F	74.19F	67.58F	68.33F	51.64F
10/11	17:00	68.87F	68.04F	67.63F	68.11F	51.41F
10/11	18:00	63.23F	62.32F	65.10F	66.07F	50.18F
10/11	19:00	58.51F	57.93F	63.15F	63.79F	48.73F
10/11	20:00	53.34F	53.64F	61.32F	61.89F	47.60F
10/11	21:00	49.75F	51.26F	59.28F	59.80F	46.43F
10/11	22:00	46.10F	48.27F	58.06F	58.52F	45.57F
10/11	23:00	44.03F	46.58F	56.67F	57.04F	44.67F
10/12	00:00	44.98F	46.95F	56.03F	56.44F	44.30F
10/12	01:00	44.71F	46.44F	55.67F	56.24F	43.96F
10/12	02:00	44.33F	46.17F	55.43F	55.89F	43.70F
10/12	03:00	41.69F	43.82F	54.69F	54.97F	43.17F
10/12	04:00	*****F	*****F	*****F	*****F	*****F
10/12	05:00	*****F	*****F	*****F	*****F	*****F
10/12	06:00	*****F	*****F	*****F	*****F	*****F
10/12	07:00	*****F	*****F	*****F	*****F	*****F
10/12	08:00	*****F	*****F	*****F	*****F	*****F
10/12	09:00	57.87F	58.66F	57.93F	58.00F	44.51F
10/12	10:00	65.68F	66.07F	60.17F	60.82F	46.66F
10/12	11:00	74.36F	74.46F	62.44F	63.16F	48.36F
10/12	12:00	78.90F	79.15F	64.19F	65.23F	49.76F
10/12	13:00	80.58F	81.08F	65.45F	66.80F	50.78F
10/12	14:00	80.35F	81.03F	66.22F	67.60F	51.42F
10/12	15:00	77.05F	77.81F	66.76F	68.06F	51.68F
10/12	16:00	73.10F	73.38F	67.40F	68.15F	51.87F
10/12	17:00	67.31F	66.31F	67.04F	67.61F	51.59F
10/12	18:00	61.62F	60.90F	64.59F	65.27F	50.04F
10/12	19:00	55.39F	55.10F	61.95F	62.46F	48.40F
10/12	20:00	50.12F	51.34F	59.53F	60.29F	47.02F
10/12	21:00	48.14F	49.81F	58.53F	59.15F	46.23F
10/12	22:00	44.47F	46.92F	56.92F	57.35F	45.31F
10/12	23:00	43.70F	45.80F	56.18F	56.22F	44.62F

Appendix II

Correlations of Experimental Data Based on Arithmetic and Weighted Average Temperatures (Table II)

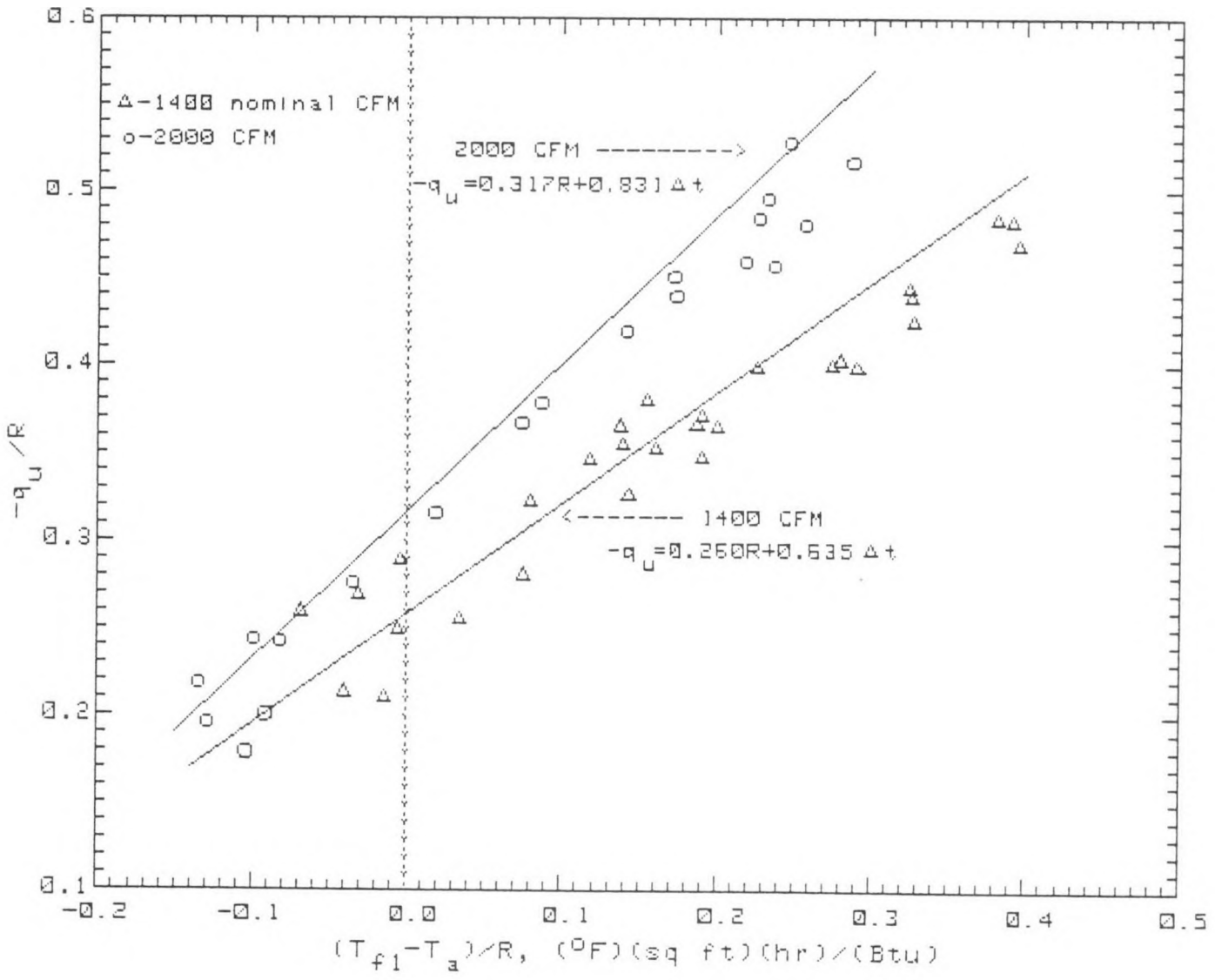

Figure 15. Correlation of experimental data using arithmetic average of outlet air temperatures.

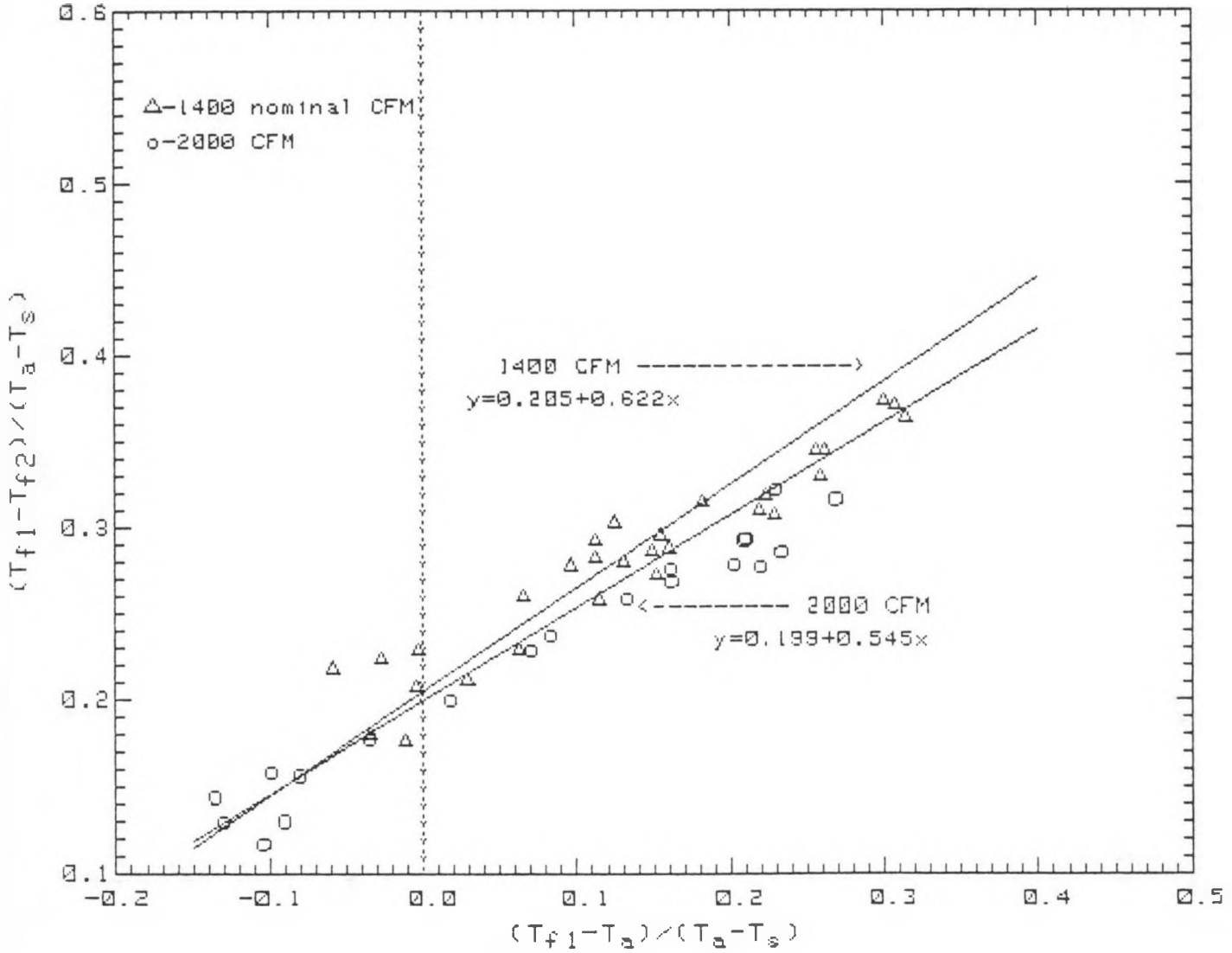

Figure 16. Alternate correlation of data using arithmetic average of outlet temperatures.

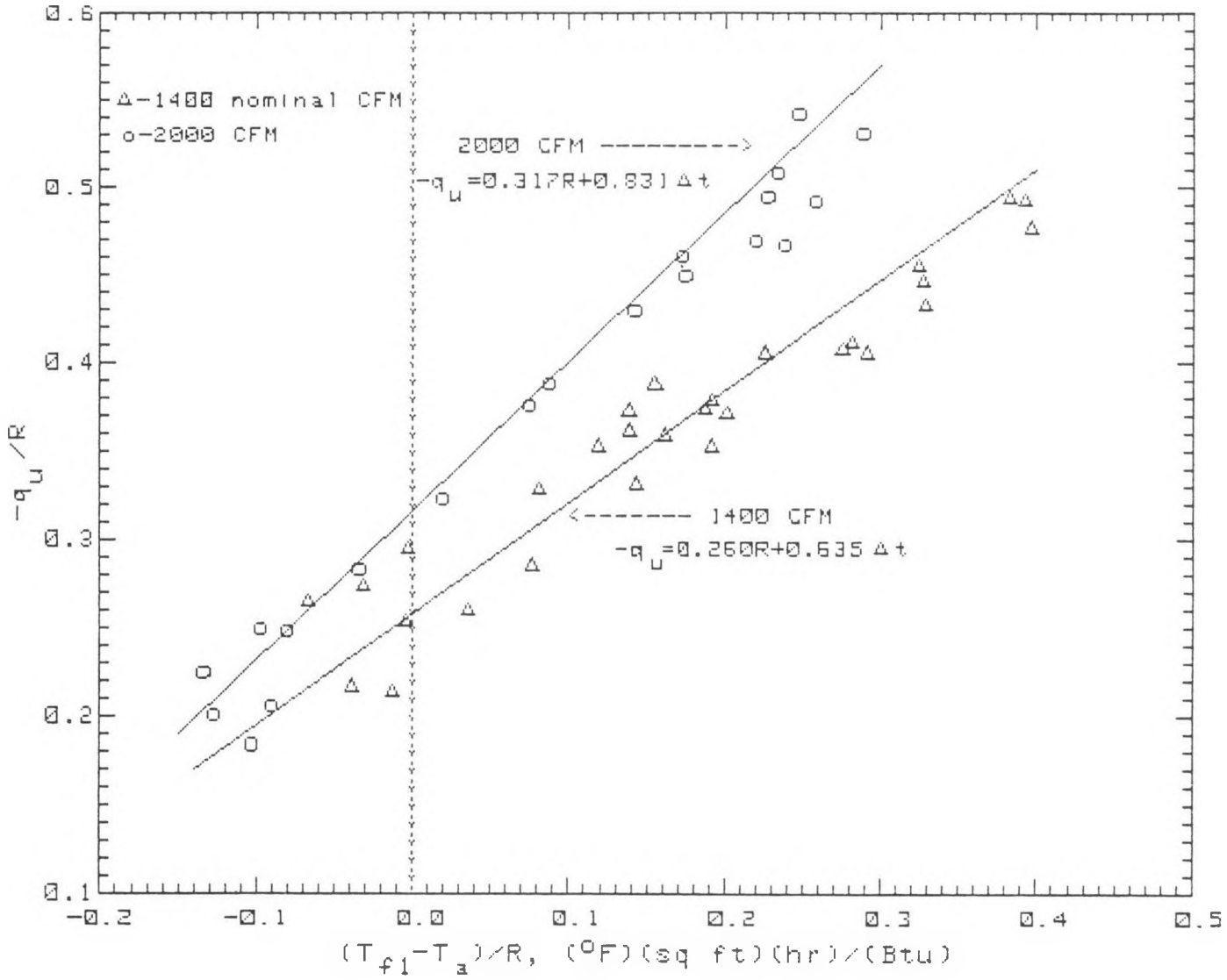

Figure 17. Correlation of experimental data using a weighted average outlet air temperature.

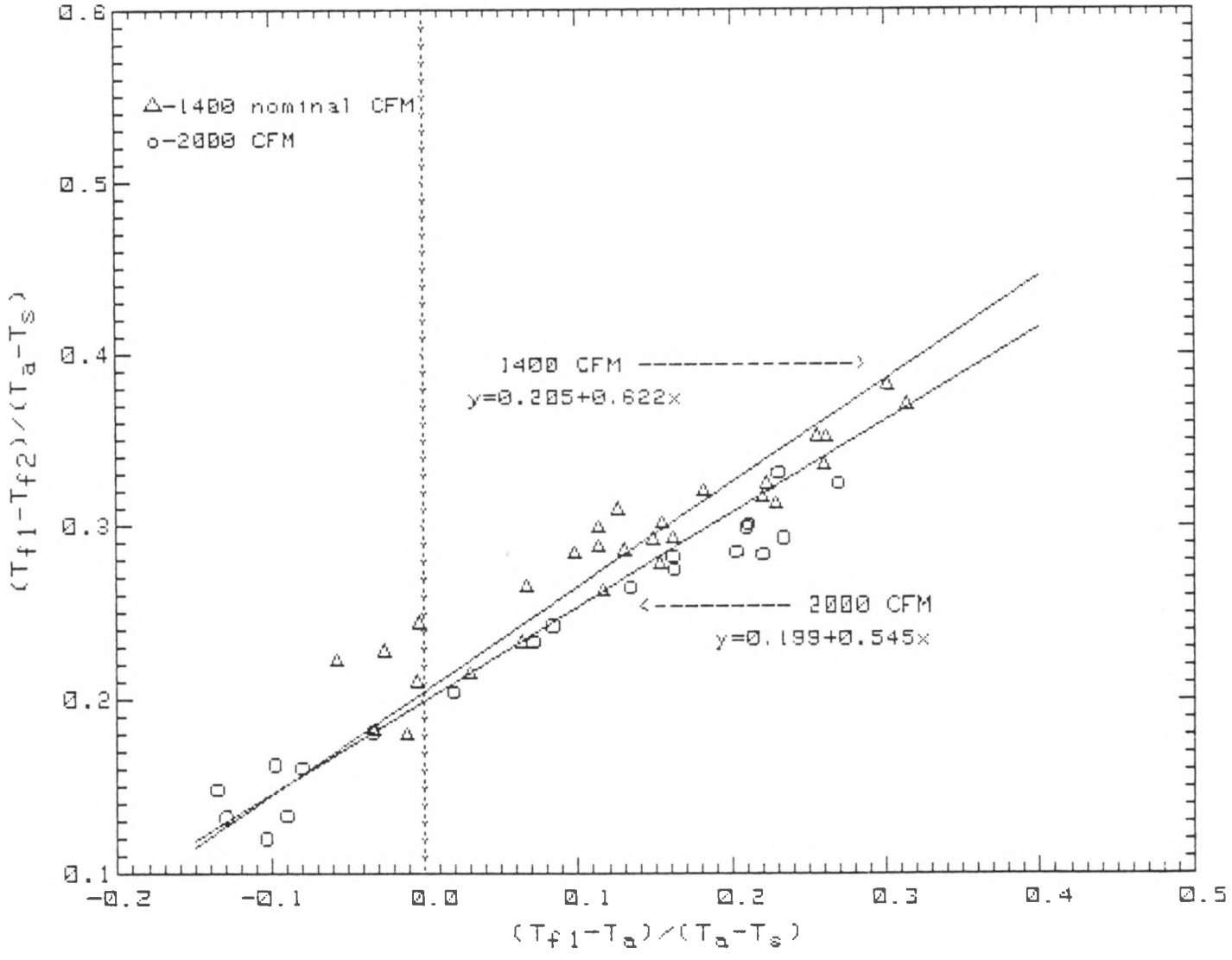

Figure 18. Alternate correlation of data using a weighted average outlet air temperature.